



DISSERTATION

Bacterial chemoreceptors: membrane boundaries and functional correlates of oligomeric state

ausgeführt zur Erlangung des akademischen Grades
eines Doktors der technischen Wissenschaften

unter der Leitung von
Univ. Prof. Dipl. Ing. Dr. techn. Peter Christian Kubicek

Institut 166
Institut für Verfahrenstechnik, Umwelttechnik und Technische Biowissenschaften

Eingereicht an der Technischen Universität Wien
Fakultät für Technische Chemie

von
DI Thomas Boldog
Matrikelnummer 9125233
Pohlgasse 54/4, 1120 Wien

Wien, 17. Mai 2006

.....
DI Thomas Boldog

Contents

Kurzfassung der Dissertation (Summary in German)	3
Summary	5
Introduction	7
1. Accessibility of introduced cysteines in chemoreceptor transmembrane helices reveals boundaries interior to bracketing charged residues	16
2. Correlation of oligomeric organization of chemoreceptors with functional activities	42
Concluding remarks	75
References	77
Curriculum vitae	85
Acknowledgements	87

Kurzfassung der Dissertation

Die Fähigkeit auf Signale in der Umgebung reagieren zu können ist eine Eigenschaft von fundamentaler Bedeutung für alle lebenden Zellen. Beispiele hierfür sind die Detektion von Licht durch Retinazellen, die Induktion von Differenzierung durch Wachstumsfaktoren oder die Bewegung von Bakterien in Richtung von Nährstoffen. Bakterielle Chemotaxis, die Bewegung von Bakterien auf Attraktans zu oder von Repellens fort, dient als Modellsystem um zu untersuchen, wie Signale in eine Zelle transduziert und in eine entsprechende Antwort übersetzt werden. Das Chemotaxissystem des Bakteriums *Escherichia coli* ist eines der best charakterisierten Signalsysteme. Entscheidende Komponente eines jeden Signalsystems sind Rezeptoren, welche verantwortlich sind für die ersten Schritte im Signaltransduktionsprozess.

Bakterielle Chemorezeptoren sind transmembrane Proteine, welche in der cytoplasmatischen Membran eingebettet sind. Die Polypeptidketten der Rezeptoren besitzen zwei Segmente, welche die Membran durchspannen, die präzisen Membrangrenzen sind allerdings nicht identifiziert. Zelluläre Signale werden sehr häufig in Phosphorylierungskaskaden durch Proteinkinasen vermittelt. Chemorezeptoren erkennen Signale in der Umgebung, vermitteln das Signal durch die Membran und kontrollieren die Aktivität einer intrazellulären Kinase. Adaption an konstante Stimuli wird bewerkstelligt wird durch kovalente Modifikation des Rezeptors. Chemorezeptoren existieren als Homodimere, es wurden aber auch höhere oligomere Zustände beobachtet und es wurde vorgeschlagen, dass höhere oligomere Zustände von Bedeutung sind für die Funktion von Rezeptoren. Eine direkte Korrelation von Rezeptorfunktion und oligomerem Zustand ist noch nicht etabliert worden.

Ziel dieser Dissertation war es, die Membrangrenzen an Chemorezeptoren zu untersuchen und den Zusammenhang zwischen oligomerem Zustand und Funktion von Chemorezeptoren zu erforschen. Die Ergebnisse dieser Arbeit erlauben es, die Membrangrenzen präzise zu definieren und eine Korrelation zwischen oligomerem Zustand und Funktion zu identifizieren. Membrangrenzen definiert durch die Versuche liegen weiter innen als von der Aminosäuresequenz erwartet. Die Ergebnisse brachten neue Information über den Aufbau von Chemorezeptoren und regen an, dass eine derartige experimentelle Untersuchung auch für andere Proteine durchgeführt wird. Nur für wenige

Proteine wurden bisher Membrangrenzen experimentell definiert, die verwendete Technik stellt eine bequeme Methode mit minimalem Eingriff dar. Die Korrelierung von Rezeptorfunktion und oligomerem Zustand brachte neue Einblicke. Sie zeigte, dass unterschiedliche Rezeptorfunktionen von Rezeptoren in unterschiedlichen oligomeren Zuständen vermittelt werden. Im Zuge der Festlegung des oligomeren Zustandes der Rezeptoren wurde eine neue Technologie adaptiert, die entwickelt wurde um Membranproteine in einer nativen Umgebung zu isolieren. Diese Technik wird von weittragender Bedeutung für die Untersuchung von Membranproteinen sein.

Summary

A feature of fundamental importance for all living cells is the ability to respond to signals from the environment. Examples of this basic property are the detection of light by retinal cells, the induction of differentiation by growth factors or the movement of bacteria towards nutrients. Bacterial chemotaxis, the movement of bacteria towards attractants and away from repellents, serves as a model system to study how signals are transduced into the cell and processed into proper responses. The chemotaxis system of the bacterium *Escherichia coli* is one of the best characterized signaling systems. Crucial constituents of any signaling system are receptor proteins which are responsible for initial steps in the signal transduction process.

Bacterial chemoreceptors are transmembrane proteins which reside in the cytoplasmic membrane. While the receptor polypeptide chains are known to have two membrane spanning segments, the precise membrane boundaries have not been identified. Cellular signaling is commonly communicated in a phosphorylation cascade through protein kinases. Chemoreceptors recognize changes in the chemical environment, mediate transmembrane signaling and control the activity of an intracellular kinase. Chemoreceptors are also involved in adaptation to constant stimuli, which is accomplished through covalent modification of the receptor. While chemoreceptors are thought to exist as homodimers, higher oligomeric states have been observed and suggested to be important for receptor function. However, a rigorous direct correlation between the different receptor functions and oligomeric state has not been established.

Aim of this thesis was to explore the location of the membrane boundaries of chemoreceptors and to investigate the relationship between oligomeric state of chemoreceptors and chemoreceptor functions. The results of this work allowed to precisely define membrane boundaries and to identify a correlation between oligomeric state and function. Membrane boundaries defined by the experiments are located interior to boundaries expected from sequence. The results provide new information about chemoreceptor organisation and suggest an experimental definition of membrane boundaries for other transmembrane proteins. Thus far membrane boundaries have been determined experimentally only for few proteins and the technique employed in this study provides a convenient and minimally perturbing approach. Correlating receptor functions

and oligomeric state provided novel insight, demonstrating that different receptor functions are mediated by receptor in different oligomeric states. In the course of defining the oligomeric state of receptors we adapted a novel technology which was recently developed to isolate receptor in a native environment. This technique will be of wide importance in studying transmembrane proteins.

Introduction

Overview

Bacterial chemotaxis, the movement of bacteria towards attractants and away from repellents, was first observed and described by Willhelm Pfeffer more than hundred years ago (Pfeffer, 1904). Since, chemotaxis of the enterobacterium *Escherichia coli* has become one of the best characterized signaling systems and has developed into an excellent model system to study signal transduction. All of the protein components involved in the signaling cascade have been identified and characterized to a high degree. It was first shown by Julius Adler that chemotaxis is mediated by transmembrane chemoreceptors (Adler 1969). Chemoreceptors are today known to play a central role not only in signal transduction, but also in adaptation. Understanding chemoreceptor structure and function is essential to elucidating the signaling process (Bren and Eisenbach 2000; Hazelbauer 2004; Wadhams and Armitage 2004).

Chemotactic Behavior

Escherichia coli is a peritrichously flagellated bacterium and moves about by rotation of its flagella (Blair 1995). In absence of chemical gradients bacteria cells exhibit a three-dimensional random walk which consists of runs in a straight line punctuated by tumbles during which the cell briefly stops and randomly reorients before swimming off in a new direction. The flagella are rotated by a protonmotive force-driven motor embedded in the cell envelope (Berg 2003). When rotated in counter clockwise direction, the flagella form a propulsive bundle and drive the cell forward in a run. A switch to clockwise rotation of one of the flagella motors causes the flagella bundle to fall apart and the cell tumbles. Tumbles interrupting runs at a constant frequency lead to three dimensional random movement. Changes in the chemical environment are sensed by the bacteria and the movement is directed to more favourable surroundings. Cells detect spatial gradients by sensing temporal changes as they swim. When an increase in attractant concentration is detected the cell suppresses the frequency of tumbling, thereby lengthening the run up the gradient. A decrease in attractant concentration or an increase in repellent concentration

has the opposite effect. Tumbling becomes more frequent, and runs in unfavourable directions become shorter. When no changes are observed, the cell adapts and resets the tumble frequency to its basal level. The control of the tumble frequency enables the cell to change the random walk into a biased walk.

Chemosensing and adaptation

The signal transduction process is initiated in the periplasm, where small molecules like sugars or amino acids, which easily pass the outer membrane, bind specifically to the periplasmic domain of a chemoreceptor, either directly or through a binding protein (Fig. 1). The chemoreceptors transmit the signal via a conformational change through the membrane (Falke and Hazelbauer 2001) to the histidine kinase CheA, which is coupled to the receptor by the scaffolding protein CheW. Receptor, CheA and CheW form a stable receptor-kinase core complex (Gegner et al. 1992; Schuster et al. 1993), additional factors, the response regulators CheY and CheB, and the methyltransferase CheR bind to the core complex to form a supermolecular signaling complex. CheA has inherent autophosphorylation activity, which is controlled by receptor in a ligand dependent fashion (Borkovich et al. 1989). Increase in attractants inhibits, decrease attractants stimulates autophosphorylation, and repellents have the opposite effect. The phosphoryl group is transferred from CheA to aspartate kinases CheY and CheB (Hess et al. 1988). Phospho-CheY diffuses to the flagellar motor, where it interacts with the flagellar switch to induce clockwise rotation and cause a tumble (Welch et al. 1993). While receptors recognize specific signals, all receptors transmit the signal to CheA and the different signals are integrated into one response. Phospho-CheY, as well as phospho-CheB, are short lived. The phosphatase CheZ enhances the inherent hydrolysis rate of phospho-CheY acting as signal terminator (Hess et al. 1988). The pair of sensor kinase and regulator kinase is referred to as two component system (Stock et al. 2000), two component systems are the predominant signaling system in prokaryotes and occur in several lower eukaryotes and plants.

The response to a change is transient, after a brief period of swimming with altered tumbling frequency the cell resumes the initial swimming pattern. Adaptation to persisting stimuli occurs through covalent modification of the receptor (Springer et al. 1979). Specific glutamates in the cytoplasmic domain are methylated by the S-

adenosylmethionine dependent methyltransferase CheR to methyl esters (Stock et al. 1984), which are demethylated by methylesterase CheB (Snyder et al. 1984). Two of the four to six modification sites are initially expressed as glutamines and deamidated to glutamates by CheB which also acts as deamidase (Kehry et al. 1983a). For their ability to accept methyl groups receptors are also referred to as methyl accepting chemotaxis proteins (MCPs). Modification is controlled by ligand, increase in attractant causes the methylation level to rise, decrease in attractant causes the methylation level to fall, and the opposite is true for repellents. Control occurs at the specific receptor, attractant occupied receptor is modified at a different rate than unoccupied receptor (Terwilliger et al. 1986b). In addition control occurs globally, since CheB is activated by phosphorylation through CheA and phospho-CheB acts on all receptors. As the modification reactions occur at a smaller time scale than the phosphorylation reactions, the modification level serves as a molecular memory of the chemical environment of the recent past. The change in receptor modification causes a change in kinase activity contrary to the change brought about by ligand and restores the receptors to the null state.

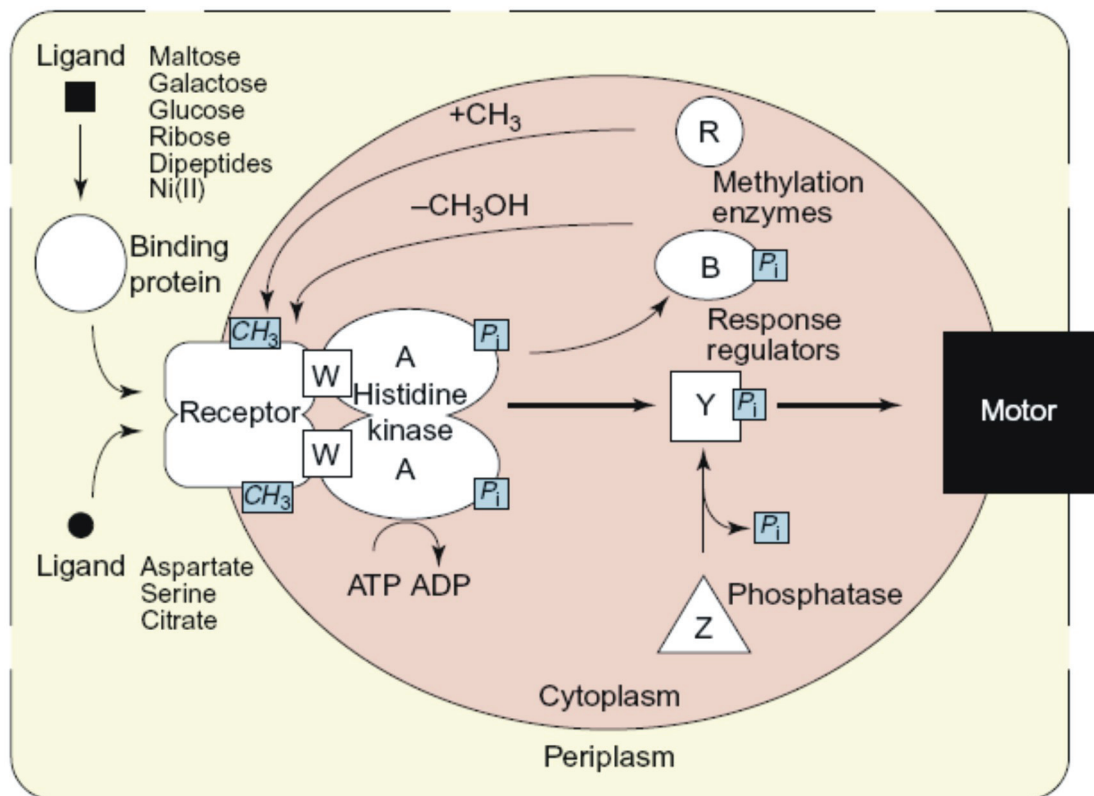


Figure 1: Chemosensory pathway. The cartoon shows the components involved in the chemosensory signaling pathway of *E. coli*. The chemotaxis Che-proteins are abbreviated by their last letters, arrows indicate the action of one component on another (Falke and Hazelbauer 2001).

Chemoreceptors

Chemoreceptors are transmembrane proteins which are embedded in the cytoplasmic membrane (Figure 2). Two identical chains with a molecular weight of about 60 kDa form a stable homodimer (Milligan and Koshland 1988). Chemoreceptors have an overall cylindrical shape with a length of 305 Å and a diameter of 30 Å (Weis et al. 2003). The periplasmic domain consists of two four helix bundles (Milburn et al. 1991), two helices of each bundle extend into the membrane forming a four helix bundle (Lee et al. 1994). The linker region is not well characterized; the cytoplasmic domain from linker to the cytoplasmic tips forms a four helix bundle (Kim et al. 1999). Four different chemoreceptors have been identified in *E. coli*: Tar mediating chemotaxis towards aspartate and maltose, Tsr recognizing serine, Trg responding to ribose and galactose and Tap mediating chemotaxis towards dipeptides. The polypeptide chains of receptors have a length of approximately 550 amino acids, the periplasmic domains have about 150 amino acids, the cytoplasmic domain approximately 320 (Bollinger et al. 1984). The periplasmic domain serves as sensor and carries the binding sites for attractants. Single amino acids bind directly to the respective receptors while dipeptides and sugars are recognized via periplasmic binding proteins. Although the periplasmic domains share low sequence homology, they have homologous structures (Lai et al. 2006). A fifth receptor, Aer, has been identified, which lacks a periplasmic domain, but has a closely related cytoplasmic domain (Bibikov et al. 1997). Aer is involved in aerotaxis, oxygen is sensed through FAD in the N-terminal cytoplasmic sensing domain of Aer. A number of compounds and environmental conditions are known to repel *E. coli*, but the repellent response is less well understood; specific repellent binding sites have not been identified. The transmembrane domain communicates binding of ligand to the periplasmic domain across the membrane via a conformational change (Falke and Hazelbauer 2001). This change is a piston type movement of one of the transmembrane helices relative to the others. The cytoplasmic domain carries the signaling domain responsible for propagation of the signal, and the methylation region responsible for adaptation. Chemoreceptors provide the framework for the supermolecular signaling complex. CheA and CheW bind to the cytoplasmic tips of the receptor, a region which is highly conserved (Le Moual and Koshland 1996). The response regulators CheB and CheY bind competitively to CheA (Li et al. 1995). The modification enzymes CheB and CheR interact not only with the methylation sites, but also with a conserved C-terminal pentapeptide on the receptor. The pentapeptide provides a

high affinity binding site for CheR (Wu et al. 1996) and serves as allosteric activator for the CheB catalyzed reaction (Barnakov et al. 2002). The pentapeptide is present only on Tar and Tsr, which are found in the cell in about 10 fold higher dosage relative to the other receptors and thus have been termed high abundance receptors (Feng et al. 1997).

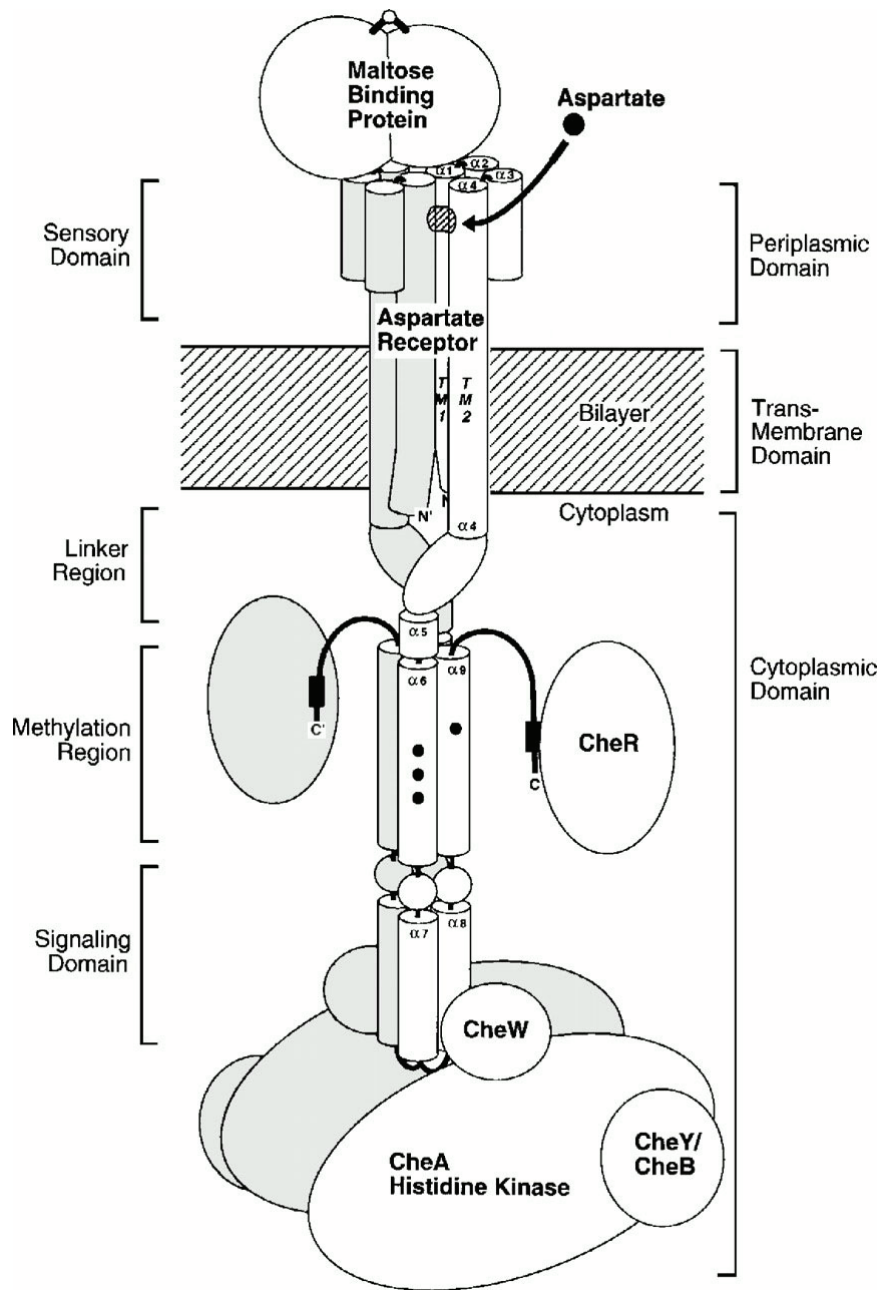


Figure 2: Signaling complex. The cartoon shows the organization of a Tar, a typical chemoreceptor, and its association with the chemosensory pathway components (Falke et al. 1997).

Membrane boundaries of chemoreceptors

Chemoreceptors possess two transmembrane segments, termed TM1 and TM2, which contain exclusively hydrophobic residues. The two segments traverse the cytoplasmic membrane as helices which form a four helix bundle (Lee et al. 1994). Transmembrane helices are commonly predicted from sequence analysis. The predictions identify stretches of residues which are predominantly or exclusively hydrophobic (Engelman et al. 1986; Rost et al. 1995), assuming that a minimum of about 20 residues is required for a canonical α -helix to span the approximately 30 Å width of the hydrophobic part of a lipid bilayer (Linden et al. 1977). TM1 and TM2 of chemoreceptor Trg have a length of 30 and 24 amino acids, respectively (Bollinger et al. 1984). This is longer than the minimum and thus the helices potentially are traversing the membrane at an acute angle to the bilayer plane or not all of the hydrophobic residues are embedded in the membrane.

Oligomeric state of chemoreceptors

Chemoreceptors form homodimers (Milligan and Koshland 1988). The ligand binding pocket is formed by the two subunits of a homodimer (Milburn et al. 1991) and transmembrane signaling occurs via a conformational change within a dimer (Falke and Hazelbauer 2001). Chemoreceptors can form trimers of dimers through interaction of the cytoplasmic tips (Kim et al. 1999; Studdert and Parkinson 2004) and the receptor-kinase complexes form large clusters at cell pole by an unknown mechanism (Maddock and Shapiro 1993). Cellular amounts of the chemotaxis proteins suggest that one trimer of dimers is in complex with one kinase dimer (Li and Hazelbauer 2004). Thus, trimers of dimers are thought to be the functional units responsible for controlling kinase activity although it has not been possible to study isolated trimers directly. It is not known if an oligomeric state higher than the dimeric state is also required for transmembrane signaling and adaptation, possibly the different functions are mediated by different oligomeric states.

Scope of this work and organization of the following chapters

Aim of this work was to investigate specific aspects of organization and function of chemoreceptors from *Escherichia coli*.

Membrane boundaries of chemoreceptors have not been determined experimentally and can only be deduced from sequence. The sequences of the transmembrane segments of chemoreceptor Trg are of different length and longer than required to span a lipid bilayer, and thus conclusions about location of the boundaries and organization of the receptor are limited. **Chapter 1** describes the experimental determination of the membrane boundaries of chemoreceptor Trg.

Chemoreceptors exist as homodimers which can form trimers and large arrays. Different functions of receptors are potentially mediated by receptor in different oligomeric states. A direct correlation of chemoreceptor function and oligomeric state has not been possible since it requires isolation of receptor in distinct oligomeric states. **Chapter 2** describes a technique to control the oligomeric state of chemoreceptor Tar and experiments to correlate oligomeric state and function.

The following chapters each consist of abstract and introduction to the specific topic, materials and methods, results, and a discussion of the observations.

1

Accessibility of introduced cysteines in chemoreceptor transmembrane helices reveals boundaries interior to bracketing charged residues

Abstract

Two hydrophobic sequences, 24 and 30 residues long, identify the membrane-spanning segments of chemoreceptor Trg from *Escherichia coli*. As in other related chemoreceptors, these helical sequences are longer than the minimum necessary for an alpha helix to span the hydrocarbon region of a biological membrane. Thus, the specific positioning of the segments relative to the hydrophobic part of the membrane cannot be deduced from sequence alone. With the aim of defining the positioning for Trg experimentally, we determined accessibility of a hydrophilic sulfhydryl reagent to cysteines introduced at each position within and immediately outside the two hydrophobic sequences. For both sequences, there was a specific region of uniformly low accessibility, bracketed by regions of substantial accessibility. The two low-accessibility regions were each 19 residues long and were in register in the three-dimensional organization of the transmembrane domain deduced from independent data. None of the four hydrophobic-hydrophilic boundaries for these two membrane-embedded sequences occurred at a charged residue. Instead, they were displaced one to seven residues internal to the charged side chains bracketing the extended hydrophobic sequences. Many hydrophobic sequences, known or predicted to be membrane spanning, are longer than the minimum necessary helical length, but precise membrane boundaries are known for very few. The cysteine-accessibility approach provides an experimental strategy for determining those boundaries that could be widely applicable.

Introduction

Much is known about the structure and structural changes of the transmembrane chemoreceptors from *Escherichia coli* (Falke and Hazelbauer 2001). However, as is the case for many transmembrane proteins, we do not know the precise boundaries of the protein segments embedded in the hydrophobic environment of the lipid bilayer. Chemoreceptors are transmembrane homodimers that are constructed of extended helical bundles (Fig. 1A). Each monomer in the homodimer has two transmembrane segments, TM1 and TM2, which traverse the cytoplasmic membrane as helices. These two regions contain sequences of exclusively hydrophobic residues longer than the ~20 necessary for a helix to span a biological membrane. For instance, the TM1 and TM2 regions of chemoreceptor Trg are defined by sequences of 30 and 24 hydrophobic residues, respectively.

Transmembrane α -helices are readily predicted in protein sequences by identification of stretches of exclusively or predominantly hydrophobic residues a minimum of ~20 residues in length (Engelman et al. 1986; von Heijne 1992; Jones et al. 1994; Rost et al. 1995). The predictions are based on the 1.5 Å distance between residues in a canonical α -helix and the ~30 Å width of the hydrophobic part of a membrane (Linden et al. 1977; Seelig and Seelig 1980; Wiener and White 1992; White and Wiener 1996). However, many hydrophobic sequences are longer than the minimum. This could reflect a transmembrane helix traversing the membrane at an acute angle and thus having more residues in the hydrophobic environment than a helix normal to the membrane, or some hydrophobic residues might not be embedded in the lipid bilayer. There are a limited number of experimental approaches for determining which specific residues along an extended hydrophobic sequence are actually embedded in the hydrophobic environment of the lipid bilayer. Some require specialized equipment and expertise (Altenbach et al. 1994) and others involve artificial fusion proteins (Monné et al. 1998; Nilsson et al. 1998). In this study we used a convenient and minimally perturbing approach combining cysteine substitutions and determination of accessibility to a hydrophilic sulfhydryl reagent to identify the membrane-embedded segments of chemoreceptor Trg.

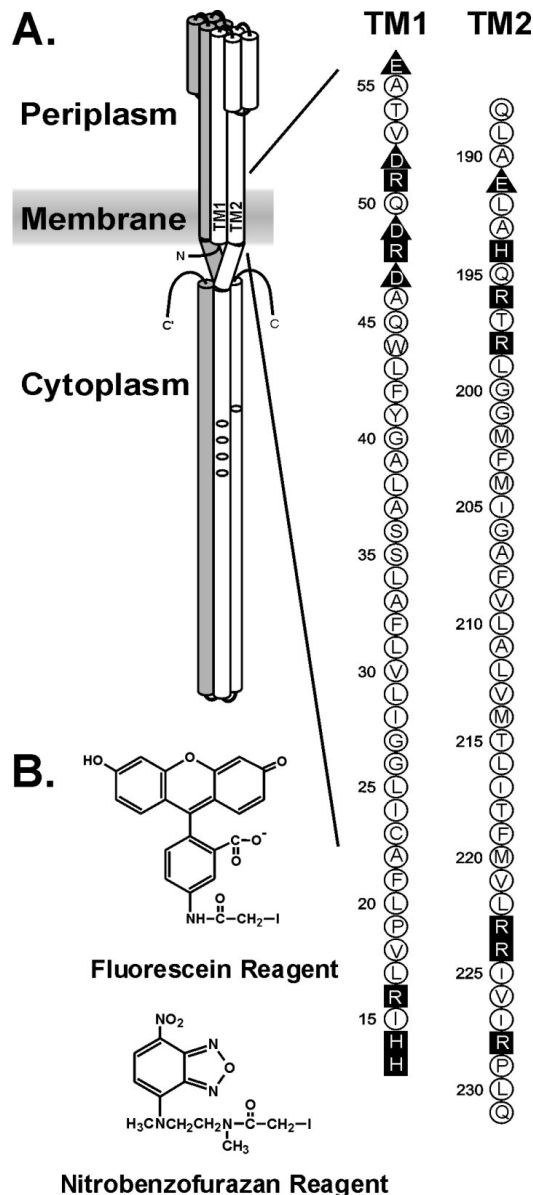


Figure 1. Chemoreceptor organization, the transmembrane regions of Trg and the fluorescent sulfhydryl reagents. A. On the left is a cartoon of the organization of a chemoreceptor homodimer. Amino (N) and carboxyl termini (C) are labeled, and one subunit is shaded. On the other subunit the transmembrane regions TM1 and TM2 are labeled and the positions of methyl-accepting sites shown by ovals. The approximate position of the cytoplasmic membrane is shown as a shaded area. On the right are the amino acid sequences (single letter code) of the TM1 and TM2 regions of Trg. Neutral and hydrophobic residues are enclosed in open circles, charged residues in dark symbols, negative charges in triangles and positive charges in squares. B. Structure of 5-iodoacetamidofluorescein (Fluorescein Reagent) and N, N'-dimethyl-N-(iodoacetyl)-N'-(7-nitrobenz-2-oxa-1, 3-diazol-4-yl)ethylene-diamine (Nitrobenzofurazan Reagent).

Materials and Methods

Single cysteine forms of Trg

We used site-directed mutagenesis (Quick Change, Stratagene) to extend the set of *trg* genes coding for single-cysteine forms of the receptor (Lee et al. 1994) to include the entire sequence from 13 through 56 and from 188 to 231. The altered genes were carried in derivatives of pGB1 (Burrows et al. 1989) or pAL1 (Feng et al. 1999) and thus were controlled by a modified *lac* promoter/operator. We introduced each plasmid into a host lacking chromosomal *trg* but otherwise wild type for chemotaxis. Growth without exogenous inducer (pGB1 constructs) or with a low concentration of inducer (pAL1 constructs) results in a cellular content of Trg comparable to that created by a single chromosomal copy of *trg* (Feng et al. 1997). We used these conditions to test the ability of each cysteine-substituted receptor to mediate chemotaxis. Strains were inoculated into a semisolid agar plate containing attractant galactose or ribose and assessed for the ability to form a chemotactic ring (Lee et al. 1995).

Membrane vesicles

The set of plasmids was introduced into CP553, which lacks chromosomal copies of *tar*, *tsr*, *trg*, *tap*, *cheB* and *cheR* (Burrows et al. 1989). To prepare membrane vesicles containing each of the single-cysteine forms of Trg, strains harboring the appropriate plasmid were inoculated into 25 mL Luria Broth containing 25 mg/mL ampicillin and incubated at 35°C with agitation. At OD₅₆₀ 0.4, isopropyl-thio-β-D-galactoside was added to 1 mM and incubation continued for 3.5 hours. Cells were harvested by centrifugation, suspended in 6 mL 100 mM sodium phosphate pH 7.0, 10 % w/v glycerol, 10 mM N,N'-ethylenediaminetetraacetic acid (EDTA), 50 mM dithiothreitol (DTT), centrifuged again, suspended in 0.9 mL of the same buffer containing freshly added 1 mM phenylmethylsulfonylfluoride (PMSF) and 1,10-phenanthroline, and stored at -20°C. Frozen cell suspensions were thawed on ice, lysed by sonic disruption (six 5 s bursts with 25 s pauses) in an ice/salt bath and centrifuged at 16,000 x g in an Eppendorf centrifuge for 10 min at 4°C. Supernatants were centrifuged 10 min, 100,000 rpm, 2°C in a TLA 100.2 rotor, the resulting pellets suspended in 950 μL 20 mM sodium phosphate pH 7.0, 2 M KCl, 10 % w/v glycerol, 10 mM EDTA containing freshly added 1 mM PMSF and 1,10-

phenanthroline, and the suspension centrifuged as previously. Pelleted membrane was suspended in 60 μL of the previous buffer lacking KCl, divided in aliquots, flash frozen in liquid nitrogen and stored at -70°C . Concentration of protein in the membrane suspensions was consistently ~ 20 mg/mL, as determined by the bicinchoninic acid protein assay (Pierce) with bovine serum albumin as the standard. Trg was $\sim 10\%$ of protein in the vesicles.

Reaction with hydrophilic sulfhydryl reagents

Frozen membranes were thawed on ice, diluted with 20 mM sodium phosphate pH 7.0, 10 % w/v glycerol, 1 mM EDTA, 200 mM NaCl to a concentration that would provide ~ 5 μM Trg in the final reaction mixture and brought to 25°C . A hydrophilic, cysteine-specific fluorescent reagent was added to the membrane suspension. For all experiments summarized in Fig. 3, the reagent was 5-iodoacetamidofluorescein (5-IAF, Molecular Probes) added to a final concentration of 500 μM from a freshly prepared 6.25 mM stock in dimethylformamide. Fluorescein carries a carboxyl group with a pK_a below 5 and a hydroxyl with a pK_a of 6.4. Thus it is negatively charged in our experimental conditions. In a few experiments, the final 5-IAF concentration was 750 μM . For some other experiments, the reagent was N, N'-dimethyl-N-(iodoacetyl)-N'-(7-nitrobenz-2-oxa-1,3-diazol-4-yl)ethylene-diamine (IANBD amide, Molecular Probes), freshly prepared in dimethylformamide. Membrane suspensions to which reagent had been added were divided into two portions and sodium dodecyl sulfate (SDS) added to one portion to a final concentration of 1 %. The SDS-treated portion was incubated 7 min at 95°C and the other portion 20 min at 25°C . Reactions were stopped by addition of 5 volumes of 40 mM trishydroxymethylaminomethane (Tris), pH 7.8, 16 mM NaH_2PO_4 , 2 % w/v SDS, 10 % w/v sucrose, 50 $\mu\text{g}/\text{mL}$ bromophenol blue, 120 mM β -mercaptoethanol. Samples were boiled for 5 min and subjected to SDS polyacrylamide gel electrophoresis in conditions that resolved the Trg band from other bands near it, specifically 11 % acrylamide, 0.073 % bisacrylamide, pH 8.2 (Kehry et al. 1983b). Immediately after electrophoresis, wet gels were analyzed for fluorescein fluorescence with a Fujifilm FLA-3000 Imaging System using 473 nm excitation illumination and a < 520 nm cut off filter. After this analysis gels were treated 1 h with the SYPRO red (Molecular Probes) fluorescent protein stain in 10 % acetic acid, destained 2 x 10 min in 10 % acetic acid and analyzed for SYPRO red

fluorescence using 532 nm excitation illumination and a <580 nm cut-off filter. The protein stain could be quantified without interference from fluorescein fluorescence because in 10 % acetic acid fluorescein is uncharged and does not fluoresce. Intensities of fluorescent bands were quantified using ImageGauge (Fujifilm) software and values adjusted for the low level of fluorescence observed for Trg lacking cysteine.

Reactivities for extra-membrane positions on both sides of the membrane (Fig. 3) greater than 0.5, and in some cases close to 1.0, indicated that the hydrophilic sulfhydryl reagent had access to both the inside and the outside of membrane vesicles. It seems likely that this reflects the incompletely sealed nature of the vesicle preparations, since it is well-documented that similar preparations exhibit receptor signaling that requires access of a charged ligand to periplasmic domains oriented in the vesicle interior (Danielson et al. 1997; Bass and Falke 1998; Butler and Falke 1998; Bass et al. 1999).

Oxidative cross-linking

Analysis of propensities for oxidative cross-linking catalyzed by Cu (phenanthroline)₃ between homologously placed cysteines in the two subunits of the Trg dimer was performed using SDS polyacrylamide gel electrophoresis and immunoblotting as described (Lee et al. 1994). Stained bands were digitized with a Kodak EDAS 290 digital camera system, intensities quantified using TotalLab (Phoretix) software. Percent cross-linking was calculated by dividing the intensity of the cross-linked dimer by the sum of the intensities of monomer and cross-linked dimer.

Results

Experimental approach

Our approach derived from one used by Falke and colleagues to characterize the extra-membrane, cytoplasmic domain of chemoreceptor Tar (Danielson et al. 1997; Bass and Falke 1998; Butler and Falke 1998; Bass et al. 1999; Falke and Kim 2000). They reasoned that substituted cysteines at positions in the native protein at which the side chain was sequestered in the protein interior should be relatively inaccessible to a bulky, water-soluble sulfhydryl reagent like 5-iodoacetamidofluorescein (Fig. 1B) but cysteines at surface-exposed positions should be relatively accessible. Their experiments revealed periodic variation in relative accessibilities that allowed identification of the helical nature of most of the ~350 residue cytoplasmic domain of the chemoreceptor (Falke and Kim 2000). Could a similar approach distinguish the membrane-embedded from the extra-membrane portions of the helices of Trg? The hydrophobic nature of the lipid bilayer should shield residues from accessibility to a polar sulfhydryl reagent, whether the side chain be packed on other elements of protein structure or exposed on the protein surface. Thus, we determined accessibility to 5-iodoacetamidofluorescein of cysteines introduced at each position within and immediately outside the TM1 and TM2 regions of Trg.

We assembled a set of 88 plasmid-borne *trg* genes coding for Trg containing a single cysteine at positions 13 through 56 and 188 through 231 (Fig. 1A). The first series included and bracketed the exclusively hydrophobic sequence from 17 through 45 that identifies the TM1 region, and the second did the same for the exclusively hydrophobic sequence from 199 through 221 that identifies the TM2 region. Of the 88 altered receptors all but one, with cysteine instead of proline at position 229, were functional as determined *in vivo* by ability to mediate chemotaxis on a semisolid agar plate. Accessibility experiments were performed by adding a fluorescent sulfhydryl reagent to membrane vesicles containing Trg and allowing the reaction to progress in two conditions, one in which the receptor was left in its native, membrane-embedded state and the other in which the detergent SDS was added, dissolving the membrane and denaturing the protein, thus providing maximal exposure of the cysteine sulfhydryl to the reagent. After these parallel reactions, samples were submitted to SDS polyacrylamide gel electrophoresis using conditions in which Trg was the only detectable protein at its position in the gel (Fig. 2). Fluorescence intensity of the Trg band was determined by scanning the untreated gel.

Then, the relative amount of protein in each Trg band was determined by treating the gel with a fluorescent protein stain and scanning it under conditions in which cysteine-coupled fluorescein did not produce a signal. For each band, intensity of fluorescein fluorescence was normalized to the relative amount of protein. Accessibility was expressed as the ratio of normalized fluorescent labeling for native, membrane-embedded receptor to normalized labeling for SDS-treated material. Values varied from 0 (no accessibility in the native protein) to 1 (identical accessibility in the native, membrane-embedded condition and in the denatured, membrane-dissolved state). Examples of primary data are shown in Fig. 2.

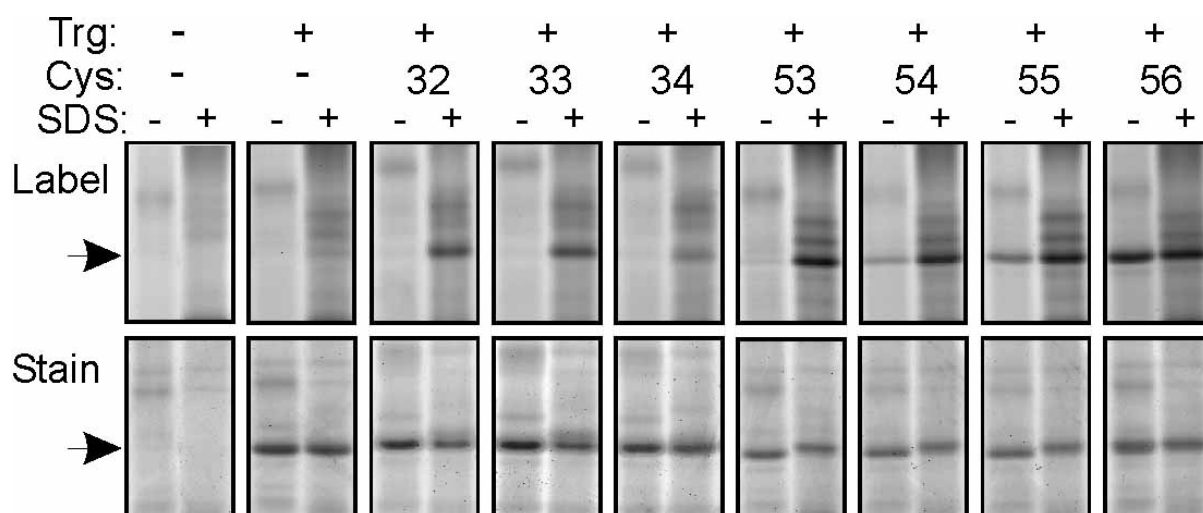


Figure 2. Labeling of cysteine-containing forms of Trg by a fluorescent sulfhydryl reagent. Trg lacking cysteine or containing a single cysteine at the indicated positions in the TM1 region was treated with 5-IAF in its native, membrane-embedded state (-) or in the presence of the denaturant and membrane solvent SDS (+), and separated from other proteins in the membrane vesicles by SDS polyacrylamide gel electrophoresis. The figure shows two fluorographic images of the same segments of SDS polyacrylamide gels, the upper ones generated by fluorescein fluorescence and the lower ones by the protein stain SYPRO red. The leftmost pairs of lanes show patterns for vesicles lacking Trg. The position of Trg, $M_r \sim 60,000$, is shown by the arrows.

Accessibility

We measured accessibility of the negatively charged, fluorescent sulfhydryl reagent 5-iodoacetamidofluorescein (5-IAF) to cysteine sulfhydryls at the 88 Trg positions using three independent membrane preparations for each position. In Fig. 3, mean values of accessibility with standard deviations are plotted by residue number for the TM1 (Fig. 3A) and TM2 regions (Fig. 3B). For both, there was an extended sequence of very little accessibility (< 0.05) to the hydrophilic reagent, flanked by sequences in which many positions exhibited substantially greater accessibility. For the regions of substantial accessibility at the periplasmic ends of both TM1 and TM2, and for much of the cytoplasmic end of TM2, low accessibility alternated with intermediate or high accessibility in a pattern consistent with helical packing. In contrast, at the cytoplasmic end of the TM1 region all positions exhibited accessibilities > 0.25 and variation in accessibility did not exhibit periodicity suggestive of a particular secondary structure.

The data identified well-resolved boundaries between hydrophobic and hydrophilic environments. At the cytoplasmic end of the TM1 region, accessibility dropped from > 0.25 for positions 13 through 21 to < 0.05 for an extended sequence from positions 22 through 40 and increased significantly beginning at position 41 (Fig. 3A). This strongly suggested that the segment of TM1 embedded in the hydrocarbon environment of the membrane was a 19-residue sequence from position 22 through 40. For the TM2 region, a continuous sequence of very low accessibilities ≤ 0.05 (positions 201 – 217) was bracketed at each end by positions with detectably increased but still very modest accessibility on the order of 0.1 (positions 200 and 218, respectively) and by adjacent positions with substantial accessibility, > 0.3 , (positions 199 and 219, respectively). Accessibility could not be determined for positions 208 and 229 because Trg with a cysteine at either position was present in vesicle preparations at a level too low for reliable measurements. Low content for Trg with cysteine at position 208 had been noted previously (Lee et al. 1995). The low content for position 229 is consistent with the inability of that protein to mediate chemotaxis (see above) and the low content of the analogous cysteine-substituted form of chemoreceptor Tar (Butler and Falke 1998). Receptors with cysteine at positions 200 or 218 were present in vesicles at relatively low levels, and thus quantification required careful definition of the extent of fluorescence above background, but it was clear that there was little accessibility at either position. Even with these limitations, the pattern of accessibilities for the TM2 region provided a straightforward conclusion: the 19-residue

sequence from 200 through 218 was the segment of TM2 embedded in the hydrocarbon membrane environment. The slightly increased accessibilities at the two ends of the sequence implied that these residues were modestly accessible to the charged reagent, perhaps as the result of subtle movements of the transmembrane helix in and out of the membrane (see Discussion).

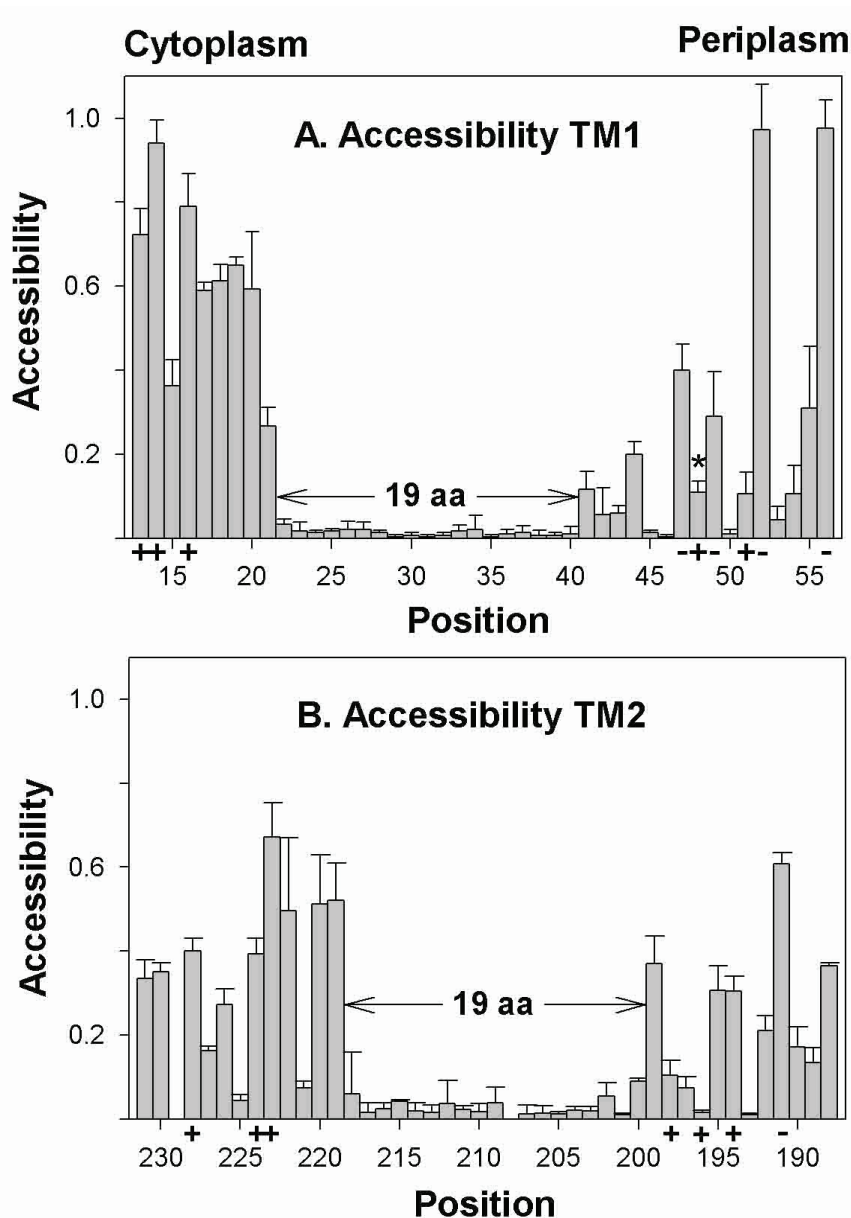


Figure 3. Accessibility of introduced cysteines to 5-IAF. Experiments like those in Fig. 2 were performed to determine relative accessibility to 5-IAF of cysteine sulfhydryls at each of the indicated positions in membrane-embedded Trg. Mean values of accessibility (three independent membrane preparations) with standard deviations are plotted by residue number from cytoplasm to periplasm for the TM1 (A) and TM2 regions (B). Positions of charged residues in the wild-type protein are marked by “+” or “-” along the abscissa and the sequence of 19 consecutive residues with minimal accessibility is marked by divergent arrows and labeled “19 aa”. Position 48 is marked by an asterisk to indicate that the low accessibility is likely the result of bracketing negative charges restricting access by the negatively charged reagent (see text). Because of low receptor content it was not possible to make reliable measurements for positions 208 and 229.

Of the four hydrophobic/hydrophilic interfaces, the periplasmic end of TM1 exhibited the least increase in accessibility on the hydrophilic side of the boundary. Studies of oxidative cross-linking between introduced cysteines (Lee et al. 1994; Hughson et al. 1997; Peach et al. 2002) (also see below) indicate that the periplasmic end of TM1 is the helical segment in the transmembrane region exhibiting closest proximity to and greatest number of interactions with neighboring helices. With close helical proximity, access of the bulky, charged 5-IAF could well be limited. We took two approaches to test this idea. In the first approach, we increased concentration and the time of exposure to 5-IAF. For the three positions on the hydrophilic side of the apparent boundary (positions 41-43) the extent of reaction increased; for three on the hydrophobic side (38-40), reaction remained unchanged and essentially undetectable (data not shown). In the second approach, we used a hydrophilic reagent that was smaller than 5-IAF and uncharged. We found that the nitrobenzofurazan sulfhydryl reagent N, N'-dimethyl-N-(iodoacetyl)-N'-(7-nitrobenz-2-oxa-1,3-diazol-4-yl)ethylene-diamine (Fig. 1B) reacted much more extensively in our standard conditions with cysteines at positions 41 and 43 (accessibility > 0.5) than did the larger, charged reagent, but still exhibited essentially no reaction for positions 38-40 (data not shown). Thus both approaches supported the location of the hydrophobic-hydrophilic boundary that had been identified by accessibility to 5-IAF in our standard conditions.

We tested accessibility of other positions on the hydrophilic side of the TM1 periplasmic boundary to the nitrobenzofurazan reagent and found a pattern of relative reactivity similar to that for 5-IAF. A striking exception was position 48, for which reactivity with the bulky, negatively charged reagent was low (Fig. 3A), but accessibility by the smaller, neutral reagent was > 0.4. This difference implied that the two negatively charged residues that bracket position 48 reduced accessibility to a cysteine that is otherwise solvent exposed.

Patterns of oxidative cross-linking

Previous studies of the hydrophobic sequences 17-46 and 199-221 had determined relative propensities for oxidative cross-linking between cysteines at homologous positions in the subunits of the Trg homodimer and thus defined helical faces of closest apposition in the transmembrane four-helix bundle (Lee et al. 1994; Hughson et al. 1997). We determined cross-linking propensities for the 88 cysteine-substituted forms of Trg contained in the three membrane preparations used for our accessibility studies (Fig. 4). Several cysteines exhibiting essentially no reactivity with 5-iodoacetamidofluorescein participated in oxidative cross-linking. Thus those cysteines were available for sulfhydryl chemistry, supporting the notion that the lack of reactivity with the charged reagent reflected a membrane-embedded location. Cross-linking results were consistent with previous studies (Lee et al. 1994; Hughson et al. 1997), and extended characterization to bordering hydrophilic regions. Extents of cross-linking across the TM1-TM1' interface exhibited a distinct helical periodicity from position 19 through 56, with local maxima defining a helical face of closest apposition between homologous helices (Fig. 5). For the portion not embedded in the membrane (41 through 56), for which variation in accessibility would be expected to reflect solvent exposure, the face of closest apposition identified by cross-linking maxima was opposite the face defined by maxima in accessibility (Fig. 5), consistent with helical packing of the periplasmic extensions of TM1 and TM1' (Peach et al. 2002). An exception was position 56, with extensive accessibility and extensive cross-linking. However, this could be understood as the consequence of the separation of subunits in this region (Milburn et al. 1991), allowing accessibility. Cross-linking propensities for positions 13 to 18 at the cytoplasmic end of the TM1 region did not exhibit periodicity and there was no correlation between accessibility and cross-linking, consistent with the model in which TM1 and TM1' splay apart toward the cytoplasm (Peach et al. 2002).

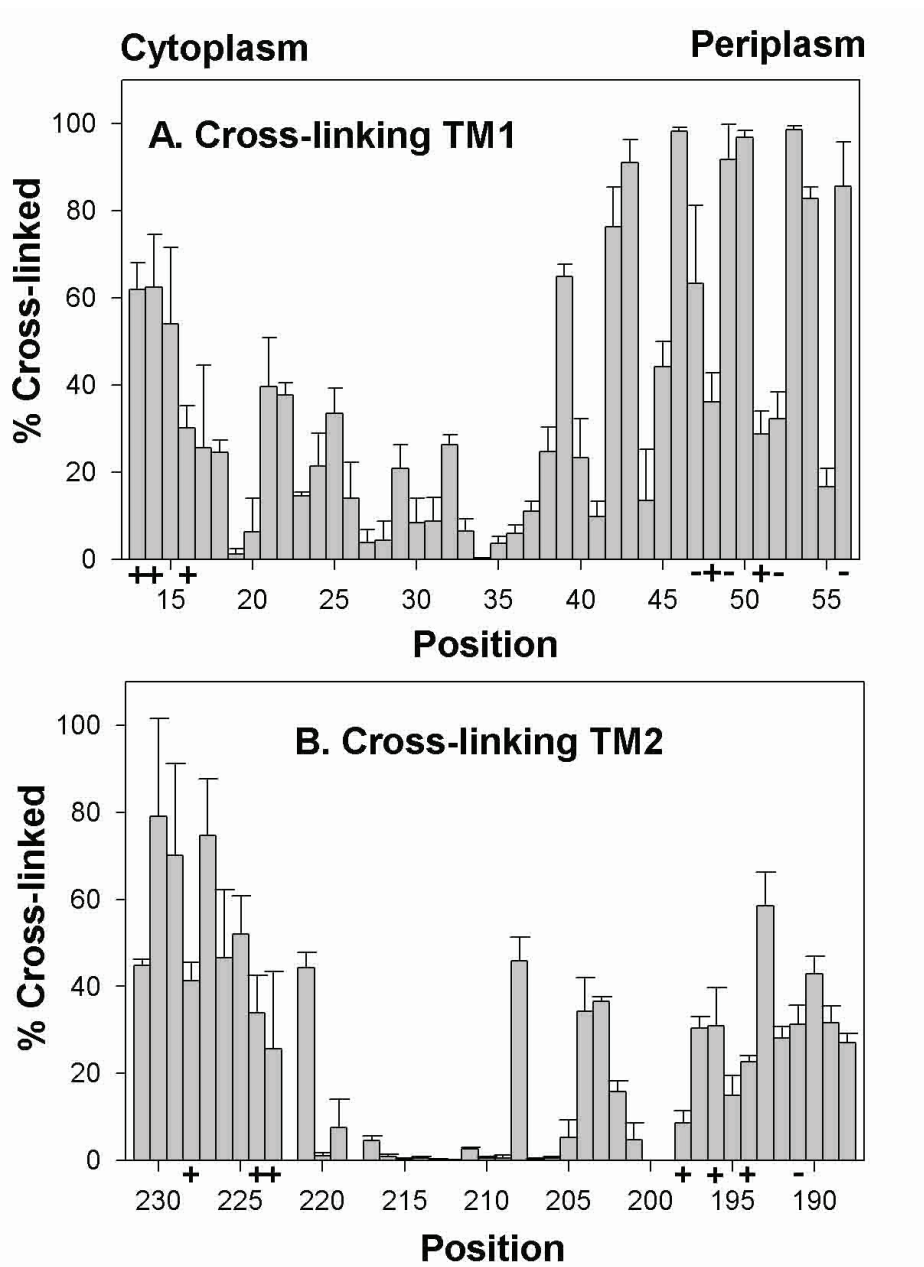


Figure 4. Oxidative cross-linking between introduced cysteines. Extent of oxidative cross-linking catalyzed by Cu (phenanthroline)₃ was determined for cysteine pairs in homologous positions in the two subunits of the Trg homodimer using the same three membrane preparations used for experiments in Fig. 3. Mean values of percent cross-linking with standard deviations are plotted by residue number displayed from cytoplasm to periplasm for the TM1 (A) and TM2 regions (B). No data is shown for positions 199, 200 and 222 because of ambiguity in the results.

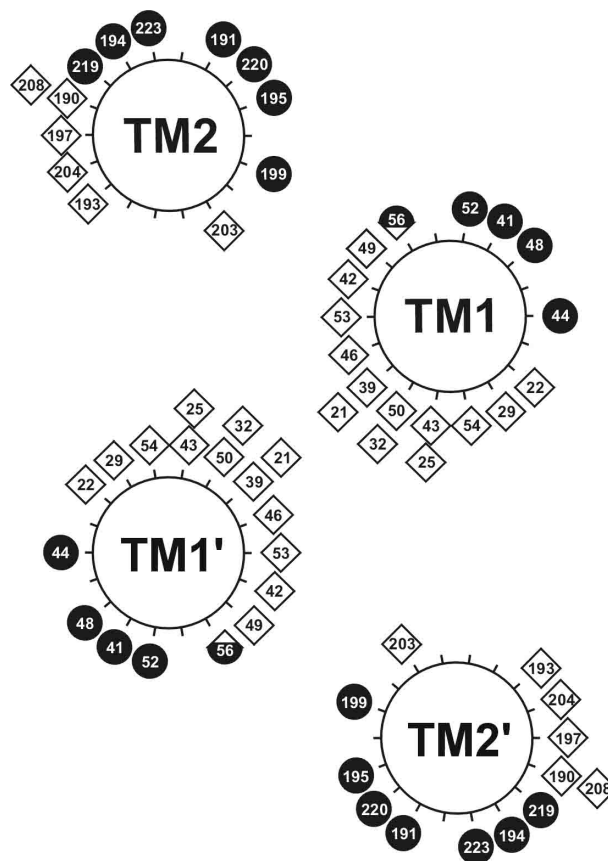


Figure 5. Distribution of maxima for accessibility and cross-linking. Local maxima for accessibility from Fig. 3 and for cross-linking from Fig. 4 are displayed as shaded circles and open diamonds, respectively, on the helical wheel diagram in the model of the Trg transmembrane domain derived from comprehensive analysis of previous cross-linking data (Lee and Hazelbauer 1995). The local maximum for position 48, which is bracketed by two negatively charged residues, represents high accessibility to an uncharged sulfhydryl reagent, not the lower accessibility for a bulky, charged reagent plotted in Fig. 3A (see text). The hybrid symbol for position 56 reflects a local maxima for both cross-linking and accessibility, created by a bulge in helical packing (see text).

For TM2-TM2', positions of local maxima in cross-linking defined a helical face of closest apposition for positions 188-208. From 209 to 220 extents of cross-linking were very low, and from 221 through 231 the pattern was not suggestive of a specific secondary structure. The only differences between the current data and the previous study (Lee et al. 1994) occurred in TM2: cross-linking was higher than observed previously at position 208 and lower at position 211. However, both sets of data identified the same helical face. For the TM2 periplasmic segment with positions accessible to the hydrophilic reagents, variation in homologous cross-linking corresponded with an opposite and complementary variation in accessibility (Fig. 5). However, in the model of the Trg transmembrane domain (Fig. 5), based on extensive cross-linking studies that included analysis of the TM1-TM2 interface (Lee and Hazelbauer 1995), the TM2 face defined by cross-linking maximal is not directly opposite the corresponding face of TM2' in the receptor dimer. This might reflect inaccuracies in the deduction of structural orientation from patterns of cross-linking. Alternatively, in an array of trimers of receptor dimers, TM2- TM2' cross-linking might occur between helices from neighboring dimers (C et al.; Studdert and Parkinson 2004).

Discussion

Boundaries of TM1 and TM2

Determination of accessibility of introduced cysteines to a hydrophilic sulfhydryl reagent provided clear identification of the segments of Trg embedded in the hydrophobic environment of the lipid bilayer. For both the TM1 and TM2 regions, there was a continuous stretch of low accessibility 19 residues long, sufficient to span the hydrocarbon environment of the cytoplasmic membrane, a distance measured some years ago as ~ 30 Å (Linden et al. 1977) and recently estimated to be ~ 27 Å (Abramson et al. 2003). At all four hydrophobic-hydrophilic boundaries, there was a distinct transition from very low accessibility to substantially higher accessibility. For TM2, the positions on the hydrophobic side of its two boundaries exhibited modestly increased accessibility, consistent with piston movements of the transmembrane helix in and out of the membrane (Falke and Hazelbauer 2001).

Relating the boundaries of two different transmembrane segments

TM1 and TM2 are parts of the same four-helix transmembrane domain, but our identification of their membrane-embedded segments did not depend on this relationship. Thus an important test was the degree to which those two segments were in register in the complete transmembrane domain. There are no high-resolution structures of the transmembrane domain of Trg, or of any other chemoreceptor. However, we have two sources of information about the relative position of TM1 and TM2, patterns of oxidative cross-linking between introduced cysteines (Lee et al. 1994; Hughson et al. 1997), and extrapolation from a model of the Trg periplasmic domain (Peach et al. 2002) created from the X-ray structure of the periplasmic domain of the related chemoreceptor Tar (Milburn et al. 1991). Utilizing these two independent sources of information provides somewhat different long-axis positioning of TM1 relative to TM2 (Peach et al. 2002). Since much evidence indicates that there is a piston motion of TM2 along this axis (Falke and Hazelbauer 2001), it seems likely that this difference reflects the natural conformational flexibility of the receptor. Precise alignment of the two 19-residue sequences of low accessibility for TM1 and TM2 of Trg places the two transmembrane helices in a register that is between the two other alignments and closer to the one defined by extrapolation

from the X-ray structure (Fig. 6). This correspondence provides confidence in the validity of our analysis and makes it unlikely that a specific cysteine substitution has altered the position of that residue relative to the membrane boundary. The combination of cysteine scanning and reagent accessibility could easily be applied to identification of membrane-embedded sequences and specific boundaries of transmembrane domains in other transmembrane proteins. Although not focusing on determination of precise membrane boundaries, the topology study of Stewart and Hermodson provides an independent example of the ability of this approach to distinguish membrane-embedded from extra-membrane positions (Stewart and Hermodson 2003).

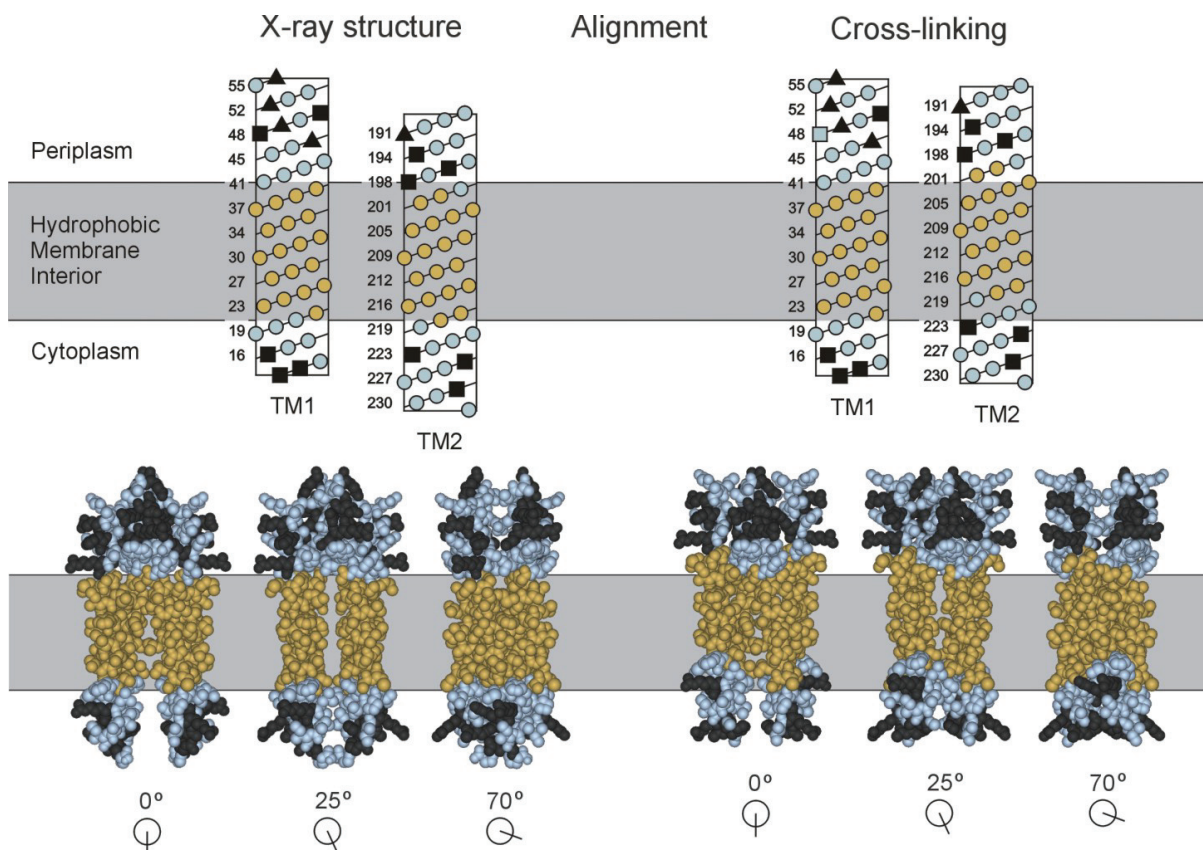


Figure 6. Alignment of TM1 and TM2. Positions in TM1 and TM2 exhibiting minimal accessibility to 5-IAF (Fig. 3) are gold and positions outside this region are blue. Charged residues, all of which are outside the region of minimal accessibility are dark gray. In the upper panel, sequences of the TM1 and TM2 regions are displayed in helical net diagrams and aligned along their long axes by two independent criteria. Left: extension of the homology model based on the X-ray structure of the periplasmic domain of chemoreceptor Tar (Milburn et al. 1991; Peach et al. 2002); right: alignment by patterns of oxidative cross-linking between introduced cysteines; (Lee et al. 1994; Hughson et al. 1997; Peach et al. 2002). The two alignments are placed relative to the membrane so that in each the minimally accessible positions in TM1 are all in the hydrophobic interior. The lower panel presents three space-filling views of the two alignments based on models of the entire transmembrane domain of Trg (Milburn et al. 1991; Peach et al. 2002). The models include TM1/TM1' residues 13 through 56 and TM2/TM2' residues 188 through 229.

Chemoreceptor organization

Nineteen-residue sequences organized as canonical α -helices should be 28.5 Å long. Thus the membrane-embedded segments of TM1 and TM2 would need to be oriented normal to the plane of the cytoplasmic membrane to span the $\sim 27 - 30$ Å width of its hydrophobic portion (Linden et al. 1977; Abramson et al. 2003). This implies that Trg, and presumably related chemoreceptors, are oriented normal to the membrane as they span it. This is the orientation shown in most diagrams and cartoons of chemoreceptors (e.g. Fig. 1). Our data provide evidence that this is the case for receptors embedded in their natural membrane environment. High-resolution electron micrographs show the same orientation for chemoreceptor Tsr in membrane fragments treated with low amounts of a non-denaturing detergent (Weis et al. 2003).

To what extent can boundaries for the Trg transmembrane domain be extrapolated to other chemoreceptors? Trg is closely related by sequence to other methyl-accepting chemoreceptors in *E. coli* and *Salmonella* (Bollinger et al. 1984) and these proteins are the most extensively characterized members of a large family of sequence-related, membrane-spanning sensory receptors found across the taxonomic diversity of bacteria and archaea (Zhulin 2001). Fig. 7 shows an alignment of the transmembrane regions of chemoreceptors from *E. coli*, *Salmonella* and the related enteric species *Enterobacter aerogenes*. In all these sequences, residues aligned with the membrane-embedded positions of Trg are exclusively hydrophobic. Thus each of these sequences could be embedded in the hydrocarbon environment of the lipid bilayer. Chemoreceptors, particularly ones as closely related as this set, are likely to have most structural features in common. Thus Fig. 7 provides a useful preliminary definition of membrane-embedded segments for other chemoreceptors.

A common feature of transmembrane helices is the presence of aromatic side chains near presumed hydrophobic-hydrophilic boundaries (Ulmschneider and Sansom 2001). Examination of sequences and suggested membrane boundaries in Fig. 7 reveals that in the set of these related chemoreceptors an aromatic side chain occurs very frequently near the periplasmic boundary of both transmembrane segments. All but Trg have an aromatic residue at the TM1 membrane-embedded position nearest the periplasm and the entire set has an aromatic side chain 3 to 5 residues from the periplasmic boundary of TM2. In contrast, among the 10 TM1 and 10 TM2 membrane-embedded sequences only 4 of 20 have aromatic residues near the cytoplasmic boundary. However, in each receptor sequence an aromatic residue occurs on the extra-membrane side of TM2 cytoplasmic boundary, at the boundary or one residue removed.

Extra-membrane segments

For the short extra-membrane segments analyzed in this study, there were local maxima of accessibility for the TM1 and TM2 periplasmic extensions (Fig. 5). The maxima defined helical faces of high accessibility and thus solvent exposure. Those helical faces were distinct from apposed helical faces defined by maxima for homologous cross-linking between introduced cysteines. Identification of a helical character for the periplasmic extension of TM2 confirmed that the $\alpha 4$ helix of the periplasmic domain (Milburn et al. 1991) is uninterrupted as it becomes TM2 (Pakula and Simon 1992; Lee et al. 1994; Lee and Hazelbauer 1995). The relatively low average values of accessibility for positions 41 through 56 and the distinct helical variation in those values were consistent with the close positioning of TM1 to TM1' and TM2 deduced from patterns of oxidative cross-linking between introduced cysteines (Lee et al. 1994; Lee and Hazelbauer 1995) and from EPR spectra of spin-labeled cysteines (Barnakov et al. 2002). In the cytoplasmic extension of TM1, positions 13-21 exhibited substantial accessibility, and the modest variation in those accessibilities was not suggestive of a specific secondary structure. In addition, extents of cross-linking between homologously placed cysteines in TM1 and TM1' positions 13-20 did not exhibit periodic variation, and there was not a reciprocal relationship between extent of accessibility and extent of cross-linking. These observations are consistent with the high mobility exhibited by EPR spin labels placed at positions 17-20 (Barnakov et al. 2002). Taken together, the data indicate there is no stable association of the cytoplasmic extension of TM1 with other elements of Trg. The sequence might be helical, but very

mobile as the result of a flexible connection with TM1 (residue 19 is a proline), or it might not maintain a fixed structure. This lack of stable association for the cytoplasmic extension of TM1 is consistent with studies of chemoreceptor Tar (Chen and Koshland 1995; Chervitz et al. 1995).

Membrane boundaries interior to bracketing charges

None of the four hydrophobic-hydrophilic boundaries we identified for the transmembrane helices of Trg corresponded to the position of a charged residue. Instead, the boundaries were displaced one to seven residues internal to the charged side chain at the ends of the extended hydrophobic sequences (specifically seven and five residues for the periplasmic and cytoplasmic ends of TM1, and one and four residues for the periplasmic and cytoplasmic ends of TM2). The displacement is notable, since charged residues are commonly found at one, and often both, ends of an extended sequence of hydrophobic residues in a putative transmembrane segment, and the frequent presence of a positive charge at the intracellular end of a transmembrane helix has provided a powerful tool for deducing topology of transmembrane helices from sequence (von Heijne 1986). A logical implication of the positive-inside rule is that the positively charged side chain would secure and stabilize the position of the hydrophobic stretch of a transmembrane helix relative to the negatively charged surface of a phospholipid bilayer. Such a role might be thought to require that the hydrocarbon-embedded portion of the transmembrane helix begin immediately adjacent to the charged residue. If this is the case, it does not appear to be crucial for the two Trg helices.

What do these observations mean? Perhaps, Trg and presumably other chemoreceptors are atypical and the displacement of the hydrophobic-hydrophilic boundary from the position of charged residues is not common but instead reflects a specific functional requirement. This could be the case for TM2 because a large body of data identifies the conformational change of transmembrane signaling in chemoreceptors as an axial sliding of that helix (Falke and Hazelbauer 2001). Hydrophobic residues at extra-membrane positions adjacent to the membrane-embedded portion of TM2 would allow axial sliding without imposing the substantial energy barrier that would have to be overcome if the membrane-embedded sequence were tightly bracketed by charged residues. However, TM1 is not thought to slide in the course of transmembrane signaling (Falke and Hazelbauer 2001), so the placement of the hydrophobic-hydrophilic boundaries

for this transmembrane segment cannot be explained in the context of a functional requirement for axial sliding.

Alternatively, displacement of hydrophobic-hydrophilic boundaries from bracketing charged residues might be relatively common for transmembrane helices, particularly in proteins with extended extra-membrane domains. At present, we do not know whether this is the case since so few hydrophobic-hydrophilic boundaries have been determined experimentally. This provides a strong motivation for applying our approach to other transmembrane helices.

2

Correlation of oligomeric organization of chemoreceptors with functional activities

Abstract

Chemoreceptors of the bacterial chemosensory system are involved in the crucial functions of ligand binding, transmembrane signaling, kinase activation and adaptational modification. While chemoreceptors have been suggested to exist and function as homodimers, increasing evidence indicates an important role of higher oligomeric states, particularly of trimers of receptor dimers. A direct correlation between the different chemoreceptor functions and oligomeric state has not been defined in a rigorous fashion. Prerequisite to address this issue is the isolation of receptors in a defined oligomeric state. We accomplished this *in vitro* by solubilizing purified receptor in nanodiscs. Inserted into nanodiscs, receptors are confined within a nanoscale disc of lipid bilayer. By controlling the number of receptor molecules inserted into a nanodisc we were able to control the number of receptor molecules available to form an oligomer. We studied chemoreceptor Tar from *Escherichia coli*; for purification purposes we employed a His-tagged variant (Tar6H). To assess the correlation between receptor function and oligomeric state we subjected receptor nanodisc preparations with a wide range in the number of receptor molecules inserted into one disc to enzymatic assays. We found that receptor in nanodiscs was competent to perform all *in vivo* activities, dependent on the oligomeric state of receptor. The lowest oligomeric state we observed is the dimeric state. Isolated receptor dimers are efficient in ligand binding, transmembrane signaling and adaptational modification, but they are not efficient in kinase activation. Optimal kinase activation requires a trimer of dimers. Dimers in a trimer of dimers exhibit the entire spectrum of functions.

Introduction

Motile bacteria are able to recognize chemicals in their environment and direct their movement accordingly, a phenomenon termed chemotaxis. The chemotaxis system of *Escherichia coli* has been extensively studied and frequently serves as paradigm for signaling systems (Hazelbauer 2004). A diagram of the chemotaxis signaling components and their interactions is provided in Figure 1. Central to chemotactic signaling are transmembrane chemoreceptors which form stable signaling core complexes with the histidine kinase CheA and the coupling protein CheW. Receptors mediate changes in the chemical environment as changes in the autophosphorylation activity of CheA. Binding of ligand to the receptor periplasmic domain inhibits CheA. The change in CheA activity is communicated to the flagellar motor by the response regulator CheY, which is phosphorylated by CheA and induces, in its phosphorylated form, a change in the direction of motor rotation. The phosphatase CheZ enhances hydrolysis of phosphorylated CheY thus acting as signal terminator. Sensory adaptation is achieved through the deamidase/methylesterase CheB and the methyltransferase CheR, which covalently modify specific side chains in the receptor cytoplasmic domain. An increase in ligand concentration speeds methylation and slows demethylation, decrease in ligand concentration has the opposite effect. While the methylation reaction is affected solely by a change in the receptor cytoplasmic domain, demethylation is further controlled by phosphorylation. CheB phosphorylation occurs through CheA and causes an enhancement of CheB activity. Receptor modification affects kinase activation. As the receptor methylation level increases, kinase activity is stimulated. The effect of the receptor modification on kinase activity is opposite to the effect by ligand which provides the mechanism for adaptation.

Chemoreceptors are known to form homodimers (Milligan and Koshland 1988), and binding of ligand occurs in a pocket formed by the subunits of a receptor dimer (Milburn et al. 1991). A large body of data suggests that the signal carried across the membrane is a conformational change which occurs within a single receptor dimer (for a review see (Falke and Hazelbauer 2001). In contrast several lines of evidence suggest a higher order organization of chemoreceptors. Immunogold labeling first showed that chemoreceptors localize, together with kinase CheA and CheW, in clusters at the cell poles (Maddock and Shapiro 1993).

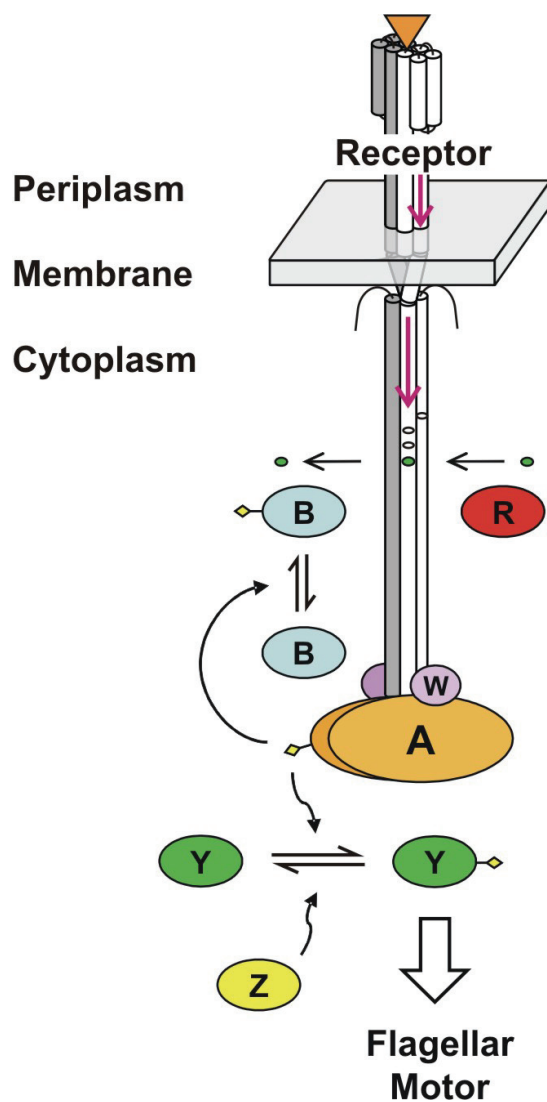


Figure 1. *E. coli* Chemosensory System. The cartoon shows all components involved in the chemosensory pathway. Chemotaxis proteins are indicated using ovals and their last letter. Receptor (white and gray cylinders) binds ligand at the periplasmic domain (orange triangle) and sends a signal (red arrows) across the cytoplasmic membrane (gray area). Kinase CheA (brown) is associated with the aid of the scaffold protein CheW (purple) with the receptor cytoplasmic tips. Autophosphorylation of CheA is stimulated by unoccupied receptor (yellow diamonds indicate phosphoryl groups) and inhibited by occupied receptor. CheA phosphorylates response regulator CheY (green), phospho-CheY docks onto the flagellar motor. Phosphatase CheZ (yellow) dephosphorylates CheY. Sites of adaptational modification (small ovals) receive methyl groups (green small ovals) by the methyltransferase CheR (red). Methyl groups are cleaved by the methylesterase phospho-CheB (blue); CheB is activated through phosphorylation by CheA.

Arrays of receptors are observed in electron micrographs of cells overexpressing receptor (Zhang et al. 2004). X-ray crystallography of a receptor cytoplasmic fragment showed the fragment organized to a trimer of dimers with receptors contacting at the cytoplasmic tips (Kim et al. 1999). The occurrence of trimers of dimers *in vivo* was demonstrated by cross-linking experiments utilizing a trifunctional cross-linker and strategically placed cysteine substitutions in the receptor cytoplasmic domain (Studdert and Parkinson 2004).

Determination of the cellular content of the chemotaxis proteins suggests a signaling core complex of one trimer of receptor dimers, one CheA dimer and two CheW monomers (Li and Hazelbauer 2004). Together these observations strongly suggest that receptor trimers of dimers form functional units which interact with CheA and CheW. However, it has not been possible to study this unit directly. It is not known if trimers of dimers are required for interaction with CheA and CheW and if the same oligomeric state is also required for transmembrane signaling and adaptation.

In the present study we aim to correlate the oligomeric organization of chemoreceptors with functional activities using a novel approach. Sligar and colleagues developed a technique to create soluble nanoscale bilayer particles termed nanodiscs (Bayburt et al. 2002). In a simple self-assembly process phospholipids and amphipathic membrane scaffold protein (MSP) assemble to a discoidal lipid bilayer fragment which is surrounded by MSP molecules (Fig. 2). The MSP chain is amphipathic and interspersed with prolines at regular distances. Two MSP molecules fold to a helical belt and encircle the bilayer disc at the lipid acyl chains. Hydrophobic side chains of MSP shield the hydrophobic acyl chains and give the particle overall hydrophilic character. Nanodiscs allow incorporation of membrane proteins and provide a way to isolate and study membrane proteins in a native-like environment in which *in vivo* protein activity is maintained (Bayburt and Sligar 2003). Moreover, nanodiscs have been successfully used to co-incorporate heterologously expressed proteins (Duan et al. 2004). We adapted this technique to study the aspartate receptor Tar from *E. coli*. Receptor nanodiscs were prepared utilizing a His-tagged variant of Tar (Tar6H) with varying numbers of receptor dimers incorporated into one nanodisc, mimicking different oligomeric states of the receptor. These preparations were subjected to assays to examine their ability for ligand binding, transmembrane signaling, kinase activation and adaptational modification.

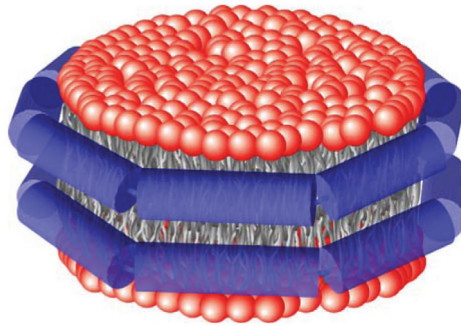


Figure 2. Nanodisc. The cartoon shows the organization of a nanodisc. Phospholipid molecules (red headgroups, gray acyl chains) are arranged in a disc of lipid bilayer. Two chains of membrane scaffold protein form a helical belt (blue cylinders) which encircles the bilayer at the lipid acyl chains.

Materials and Methods

Bacterial strains and plasmids

Tar6H was expressed from plasmid pAL67 in strain RP3098. RP3098 is a derivative of *E. coli* K 12 carrying a deletion from *flhA* through *flhD* and does not produce any Che proteins or receptors (Parkinson and Houts 1982). Plasmid pAL67 carries the gene encoding for Tar with six histidines added to its carboxyl terminus under the control of a modified *lac* promoter and a *lacI^f* gene (Lai and Hazelbauer 2005).

Growth of Bacteria and Preparation of Receptor Containing Membrane Vesicles

Preparation of inner membrane vesicles was carried out in essence as described by (1994), based on the method of (1974). All cultures were grown in Luria Broth in presence of 100 µg/mL ampicillin at 35°C under agitation. 2.4 L of media were inoculated to a starting OD₅₆₀ 0.05 from precultures in late log phase (OD₅₆₀ ≤ 1.0). At OD₅₆₀ 0.4 expression was induced by addition of isopropyl-thio-β-D-galactoside to 1 mM and incubation was continued. Growth was stopped 3.5 h after induction (OD₅₆₀ ≈ 4.2) under aeration by swirling the flasks on ice. Cells were harvested by centrifugation for 10 min at 8,000 rpm and 4°C in a SCL-6000 rotor. Cell pellets were suspended in 30% sucrose, 10 mM Tris·HCl, pH 8.0, 5 mM EDTA on ice, and the volume was adjusted to 100 mL (OD₅₆₀ 100). Subsequent steps were carried out at 8°C. Lysozyme was added from a freshly prepared solution to 100 µg/mL and the suspension was incubated for 30 min while slowly stirring. Thereafter 200 mL of 5 mM EDTA, pH 8.0, 1 mM PMSF were added at 5 mL/min to prepare spheroblasts. Quickly 1.2 L H₂O were added to lyse the spheroblasts. Released DNA was digested by adding DNase1 to 10 µg/mL and MgCl₂ to 2 mM and incubating for 20 min. Membranes were harvested by centrifugation for 2.5 h in a GSA rotor at 12,500 rpm and 4°C. Six density gradients were poured with sucrose solutions, which were prepared in 5 mM Tris·HCl, pH 8.0, 5 mM EDTA, in thin-walled SW32 tubes as follows: 5 mL 55% sucrose, 11 mL 50% sucrose, 5 mL 45% sucrose, 6 mL 40% sucrose, 6 mL 35% sucrose. Membrane pellets were suspended in 30% sucrose, 10 mM Tris·HCl, pH 8.0, 5 mM EDTA, brought to 30 mL and layered in 5 mL portions onto the gradients. Gradients were centrifuged at 32,000 rpm and 4°C in a SW32 rotor for 14-16 h. Inner membrane vesicles formed a band at 46% sucrose and were harvested with a Pasteur pipette.

Membranes were diluted with H₂O to ~10% sucrose and pelleted by centrifuging for 1 h at 60,000 rpm and 4°C in a 60Ti rotor. Membranes were suspended in 50 mM Tris·HCl, pH 7.5, 10 % w/v glycerol, and stored at -70°C after freezing in aliquots in liquid N₂. Total protein concentration was determined using the bicinchoninic acid assay; receptor concentration was determined by immunoblotting using a standard of known concentration.

Purification of Receptor

Tar6H membranes were put on ice and thawed by adding 50 mM Tris·HCl, pH 7.5, 10 % w/v glycerol at room temperature and thereby diluted to ≤ 10 mg/mL total protein. Membranes were solubilized by adding β -octylglucoside at a ratio of 1% w/v β -octylglucoside per 1 mg/mL total protein and incubated on ice for 10 min. Solubilization was carried out in presence of 2 μ M leupeptin, 2 μ M pepstatin, 1 mM phenylmethylsulfonyl fluoride (PMSF) and 100 μ M N α -p-Tosyl-L-lysine chloromethyl ketone hydrochloride (TLCK). Unsolubilized material was pelleted by centrifugation in a TLA 100.4 rotor at 100,000 rpm and 4°C for 15 min. The supernatant was loaded to a Ni-NTA agarose column (Quiagen) with 8 mL bed volume, which was equilibrated in 50 mM Tris·HCl, pH 9.0, 10 % w/v glycerol, 100 mM NaCl, 25 mM cholate, 15 mM imidazole. After washing with 5 column volumes of equilibration buffer receptor was eluted with 5 volumes 50 mM Tris·HCl, pH 9.0, 10 % w/v glycerol, 100 mM NaCl, 25 mM Na-cholate, 300 mM imidazole. Eluted sample was concentrated approximately 10 fold using Centriprep contractors with 30,000 MWCO. Concentrated sample was dialyzed three times, each time 8-12 h against 100 volumes of 50 mM Tris·HCl, pH 7.5, 10 % w/v glycerol, 25 mM cholate using Spectra/Por tubing with 12-14,000 MWCO and 6.4 mm inner diameter. The preparation was frozen in aliquots in liquid N₂ and stored at -70°C. Receptor concentration was determined by SDS-PAGE using Tar6H of known concentration.

Membrane Scaffold Protein (MSP)

MSP was kindly provided by Steve Grimme. For all experiments MSP1D1E3(-) was used (Denisov et al. 2004). The lyophilized powder was reconstituted in H₂O to yield a solution of approximately 4.5 mg/mL in 20 mM Tris·HCl, pH 7.4, 100 mM NaCl, 0.5 mM EDTA,

0.01% NaN₃. The solution was passed through a 0.2 μm filter and stored at +4°C. MSP concentration was determined spectrophotometrically at 280 nm using $\epsilon = 0.868 \text{ mL mg}^{-1} \text{ cm}^{-1}$.

Solubilization of lipids

E. coli lipids were purchased in form of chloroform stocks (Avanti). Aliquots were placed in glass tubes and the solvent was removed with a gentle stream of N₂ while rotating the tube, creating a thin lipid film. The lipid film was dried over night in a vacuum desiccator. Solubilization buffer, 50 mM Tris·HCl, pH 7.5, 100 mM Na-cholate, was added to reach the original volume, the tubes were flushed with N₂ and sealed with parafilm. To hydrate the lipid film the tubes were agitated at 200 rpm and 35°C for 2 h. For complete solubilization the suspensions were sonicated in 6 cycles of 5 s sonication and 25 s pause using a Tekmar TM-250 sonic disruptor equipped with a microtip at output 2. The solution was passed through a 0.2 μm filter and stored at -70°C. Before freezing tubes were flushed with N₂.

Nanodisc preparation

Purified Tar6H, MSP and lipids were combined and incubated by rocking for 1 h at room temperature in presence of 1 mM PMSF, 1 μM leupeptin and 1 μM pepstatin. Care was taken to keep the cholate concentration above 25 mM to maintain receptor and lipid solubility. Tar6H concentration was 10 μM in all preparations. The nanodisc components MSP and lipid were kept at a constant molar ratio of 1:120 for all preparations. The ratio of receptor to nanodisc components was adjusted as desired. Detergent was removed by incubation with BioBeads SM-2 (BioRad). To 1 volume of assembly mixture 2/3 volume BioBeads hydrated in H₂O were added and the mixture was incubated 1 h by rocking at room temperature. BioBeads were removed by centrifugation for 1 min at 3,700 rpm in a GH 3.8 rotor. The solution was loaded to a Ni-NTA agarose column, with a bed volume equal to the volume of the assembly mixture, equilibrated in 50 mM Tris·HCl, pH 9.0, 10 % w/v glycerol, 100 mM NaCl, 15 mM imidazole. The column was washed extensively with 12-15 column volumes of equilibration buffer, and nanodiscs were eluted with 5 column volumes of 50 mM Tris·HCl, pH 9.0, 10 % w/v glycerol, 100 mM NaCl, 300 mM imidazole. Eluted sample was concentrated using AmiconUltra 4 concentrators with

30,000 MWCO. Concentrated sample was dialyzed using Spectra/Por tubing with 12–14,000 MWCO and 6.4 mm inner diameter, in three steps, each 8-12 h against 100 volumes of 50 mM Tris·HCl, pH 7.5, 10 % w/v glycerol, 100 mM NaCl, 0.5 mM EDTA. Nanodisc preparations were frozen in liquid N₂ and stored at -70°C. Concentration of Tar and MSP were determined by SDS-PAGE using standards of known concentration.

Size exclusion HPLC

High performance liquid size exclusion chromatography was performed on a TSK G5000 PW_{XL} column (7.8 mm inner diameter x 30 cm, Tosho Haas) in 50 mM Tris·HCl, pH 7.5, 10 % w/v glycerol, 100 mM NaCl, 0.5 mM EDTA at 19°C. Flow was 0.7 mL/min and 0.3 mL fractions were collected.

Receptor modification assays

In vitro methylation and deamidation assays were adapted from (Barnakov et al. 1999). All assays were performed at room temperature in 50 mM Tris·HCl, pH 7.5, 10 % w/v glycerol, 2 mM DTT, 0.5 mM EDTA (TEDG). To test for maximal modification high enzyme concentrations were used and the extent of modification after 30 min incubation was determined by immunoblotting. For methylation, receptor preparations were combined with CheR lysate and S-adenosyl methionine (SAM, Amersham) to the following final concentrations: 2.5 μM receptor, 5 μM CheR, 50 μM SAM. For deamidation receptor preparations were incubated with purified CheB and phosphoramidate (PA, see below) at 2.5 μM receptor, 5 μM CheB and 50 mM PA in presence of 25 mM MgCl₂ and 10 mM KCl. Reactions were stopped by addition of SDS-sample buffer and samples subjected to SDS-PAGE designed to resolve different receptor modification states (11% acrylamide, 0.073% bisacrylamide, pH 8.2, (Kehry et al. 1983b)). Receptor bands were visualized through immunoblotting with anti-Tar serum. To test for the effect of ligand on modification, the methylation assay conditions were adjusted to allow determination of initial rates using [³H]-SAM (Amersham) and scintillation counting. CheR was used at 0.15 μM and SAM at 50 μM, parallel reactions were performed in presence and absence of 1 mM aspartate. At various times, aliquots were removed and the reaction was quenched with SDS-sample buffer. The proteins were

resolved on 10 % SDS-gels and the radioactivity of the receptor band was determined using the vapour diffusion assay (Chelsky et al. 1984).

Synthesis of phosphoramidate

Phosphoramidate was prepared by aminolysis of POCl_3 as described by (Sheridan et al. 1971). 0.2 mol POCl_3 (18.3 mL) were added dropwise to 1.5 mol NH_3 (300 mL 10% NH_3) while stirring on ice, after the last addition stirring was continued for 15 min. 1L acetone was added and, after stirring for 1 min, phases were allowed to separate. The pH of the water phase was adjusted to 6.0 using glacial acetic acid. Precipitate was collected by centrifugation for 5 min in a GH 3.8 rotor at 3,500 rpm and 4°C. The product was washed with EtOH and dried under vacuum. Note: we found that the additional precipitate which can be obtained by diluting the water phase with EtOH did not activate CheB and thus we omitted this step.

Protein phosphorylation assays

Phosphorylation was assayed *in vitro* in coupled assays which were performed in essence as described by (Barnakov et al. 1998). To form signaling complexes receptor preparations were incubated with CheA, CheW and CheY in TEDG buffer in the presence of MgCl_2 and KCl for 1 h at room temperature. Phosphorylation reactions were initiated by addition of [γ - ^{32}P]-ATP (Amersham, ~6000 cpm/pmol) yielding the following assay concentrations: 2.5 μM receptor, 0.25 μM CheA, 4 μM CheW, 10 μM CheY, 0.4 mM ATP (~600 cpm/pmol), 5 mM MgCl_2 and 50 mM KCl. Parallel reactions were performed in presence and absence of 1 mM aspartate. After 15 s reactions were stopped by addition of 4x SDS-sample buffer containing 75 mM EDTA. Proteins were resolved on 15% SDS-gels. Phospho-CheY bands were visualized and quantified by phosphorimaging.

Results

Receptor-Nanodisc Preparation

We aimed to isolate chemoreceptor Tar in a way which would capture chemoreceptors in different oligomeric states in order to investigate the correlation between oligomeric state and the different receptor functions. For this purpose we solubilized receptor Tar in nanodiscs. Nanodiscs are discoid pieces of lipid bilayer which can be generated at a defined size (Denisov et al. 2004). To assemble nanodiscs membrane scaffold protein (MSP) and detergent solubilized lipid are combined. Upon removal of detergent, nanodiscs form in a simple self-assembly process (Bayburt et al. 2002). In nanodiscs, lipid is arranged in a disc of lipid bilayer and MSP encircles the bilayer disc at the lipid acyl chains. Membrane protein present in the assembly mixture is incorporated into the nanodiscs. In this fashion nanodiscs allow purification of a membrane protein in a native-like environment (Bayburt and Sligar 2003). Bayburt and Sligar described the preparation of bacteriorhodopsin containing nanodiscs from purified bacteriorhodopsin in Tritin X-100, a MSP variant, which carries a hexa-His tag, and dimyristolphosphatidylcholine (DMPC) solubilized in cholate. We adapted their procedure to prepare receptor containing nanodiscs. We used Tar, engineered to carry a C-terminal hexa-His-tag (Tar6H), purified in cholate, a longer MSP variant, which produces a larger disc and which does not carry a His tag, and *E. coli* lipids solubilized in cholate. The principle is illustrated in Figure 1. The components are combined and incubated. Detergent is removed by incubation with BioBeads and nanodiscs form. Nanodiscs which did not incorporate receptor are separated from receptor nanodiscs by affinity purification using the hexa-His-tag on Tar6H and Ni-resin. The process is monitored by SDS-PAGE analysis of samples at each step of the procedure as displayed in Figure 3. Tar6H and MSP are shown as they are combined in detergent with lipid. After removal of detergent, bulk of receptor is found in solution together with MSP. Receptor binds to the affinity column, excess of MSP, which does not carry an affinity tag, is washed off the column. A significant portion of MSP is retained and co-elutes with receptor.

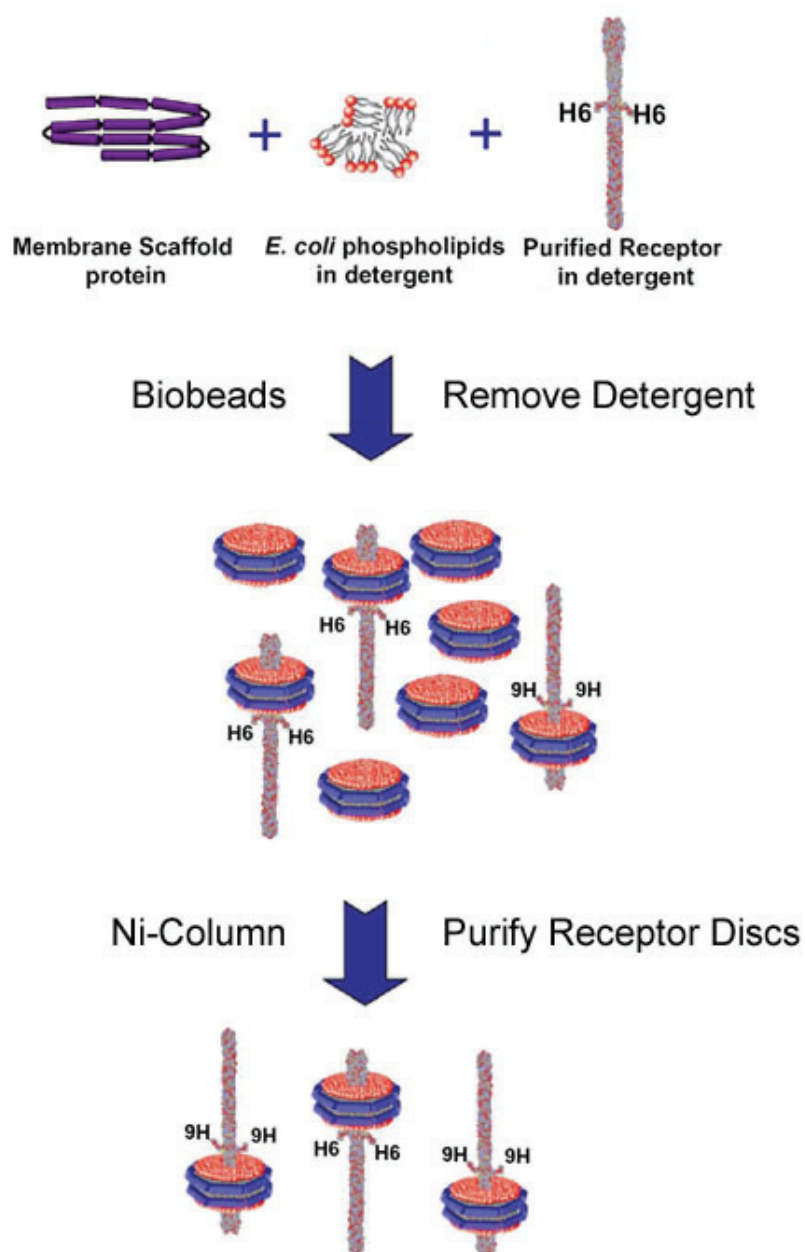


Figure 3. Receptor Nanodisc Preparation Scheme. The nanodisc components, membrane scaffold protein and *E. coli* phospholipids, solubilized in detergent are combined with purified receptor in detergent. Upon removal of detergent with BioBeads, nanodiscs form with receptor incorporated into the lipid bilayer. Receptor containing nanodiscs are purified on a Ni-column utilizing the His-tag on the receptor.

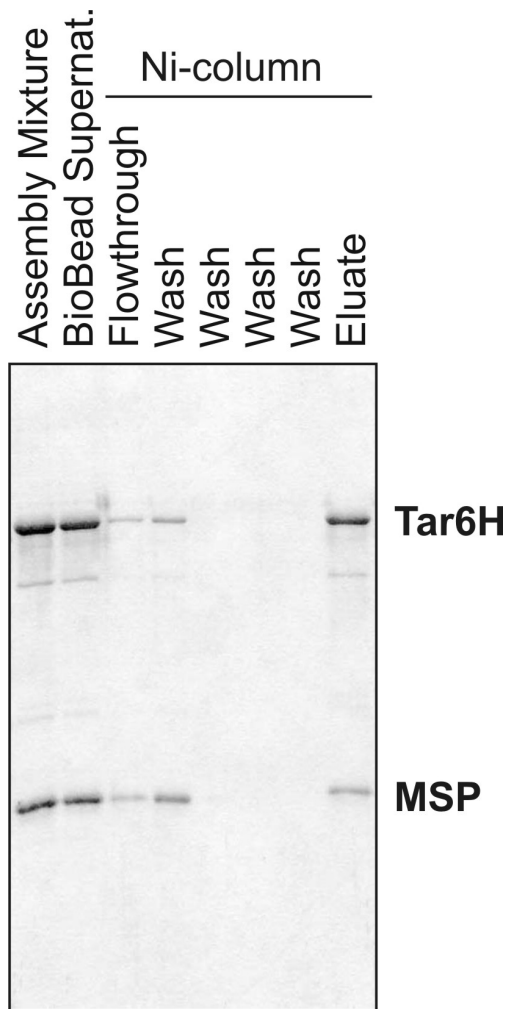


Figure 4. Receptor Nanodisc Preparation. Samples were taken during each nanodisc preparation at indicated steps and analyzed by SDS-PAGE. Positions of Tar6H (60 kDa) and MSP (30 kDa) are indicated to the right.

The successful formation of Tar nanodiscs was tested by size exclusion HPLC. Incorporation of the long, cylindrical receptor dimer into a nanodisc would be expected to cause a significant increase in the hydrodynamic radius of a nanodisc. Thus in size exclusion chromatography Tar discs would be expected to elute earlier than nanodiscs which do not have receptor incorporated. In consecutive runs we injected nanodiscs and nanodiscs prepared in the presence of receptor. The profiles of these runs are shown in Figure 2A. Indeed Tar nanodiscs elute earlier than nanodiscs without protein incorporated. SDS-PAGE analysis of the size exclusion fractions, as pictured in Figure 2B, confirms that MSP in the Tar disc sample elutes earlier than MSP in the disc sample. MSP and Tar co-elute in Tar discs. The peak of MSP appears slightly delayed relative to the Tar peak and trails which is most likely due to the presence of a small amount of empty discs.

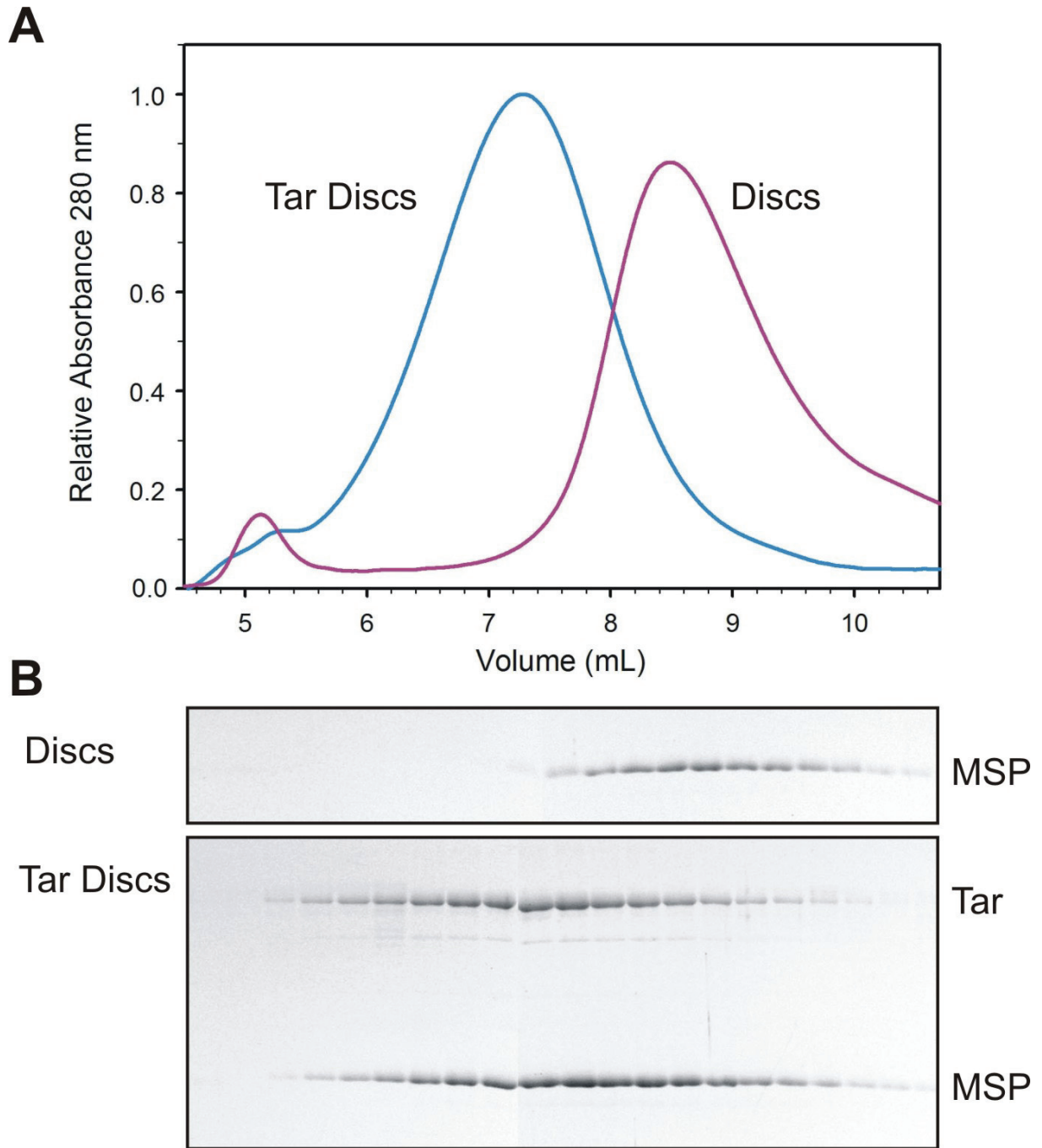


Figure 5. Size Exclusion Chromatography. Upper panel (A): Chromatograms of two consecutive injections of nanodiscs and Tar nanodiscs onto a size exclusion column (TSK G 5000) column. Lower panel (B): SDS-PAGE analysis of fractions from size exclusion; position of the proteins are indicated to the right. Note: amounts injected were chosen to result in similar absorbance; amounts loaded to the gel were adjusted to result in similar band intensities.

Controlling the Number of Receptor Molecules per Nanodisc

Nanodiscs provide a patch of lipid bilayer of defined size. The size of the nanodiscs can be controlled by the length of the MSP protein (Denisov et al. 2004). We chose MSP1D1E3(-) for our preparations. Nanodiscs prepared with this MSP variant have an overall diameter of 128 Å and a thickness of 53 Å. The lipid bilayer portion of the nanodisc has a diameter of about 105 Å. Receptor dimers have an overall cylindrical shape of 30 Å diameter and 305 Å length. The cylinders insert into the membrane with the cylinder axis approximately perpendicular to the bilayer plane. The periplasmic and cytoplasmic domains of the receptor have a length of 61 Å and 191 Å, respectively (Weis et al. 2003). Using these dimensions we modelled receptor dimers into nanodiscs. Figure 6A and 6B show nanodiscs with one receptor dimer incorporated in top and side view with the molecular dimensions indicated. Nanodiscs of this size would be expected to be able to accommodate maximally 7 receptor dimers, as modelled in Figure 6C. Preparation of receptor nanodiscs with 1-7 receptor dimers incorporated possibly allows to capture receptor oligomeric states ranging from a simple dimer up to a heptamer of dimers. We tested if the number of receptors per disc could be controlled by adjusting the input into the assembly mixture. The input ratio of Tar to MSP was varied over a wide range. For the different assembly mixtures, Tar was kept at the same concentration and the disc constituents MSP and lipid were kept at constant ratio, the ratio of Tar and disc constituents was altered. For each preparation the ratio of Tar and MSP was determined by SDS-PAGE. The relationship between the input ratio Tar/MSP in the assembly mixture and the output ratio Tar/disc in purified nanodiscs is shown in Figure 7. The number of receptor molecules can be well controlled by adjusting the input ratio. At excess of MSP the output ratio is constant at 2 Tar/disc supporting the notion that receptors insert as dimers which do not dissociate. Receptor dimers do not associate to an oligomeric state higher than dimer before they are inserted into a nanodisc; receptors insert independently. We obtained output ratios which were not integral which is consistent with independent insertion of dimers. Not a single species of receptor discs with one exact output ratio is generated, but rather several species with a distribution of Tar/disc ratios. The determined output ratio reflects the average composition of a preparation.

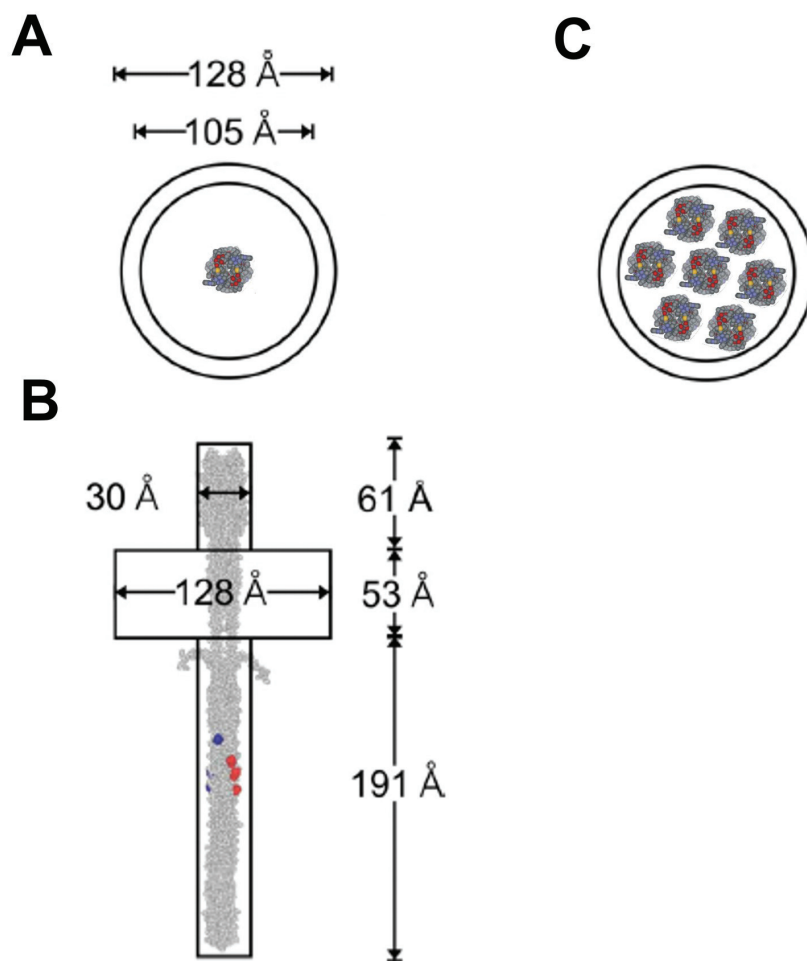


Figure 6. Receptor Nanodiscs Models. Receptor nanodisc models were created from molecular dimensions of receptor (Weis et al. 2003) and nanodisc (Denisov et al. 2004), as indicated. Receptor is represented in CPK (using coordinates from (Kim et al. 2002)). Panel (A) and (B) display a nanodisc with one receptor dimer incorporated in top and side view, respectively. Panel (C) shows a nanodisc with the maximum number of receptor dimers (7 dimers) fitted.

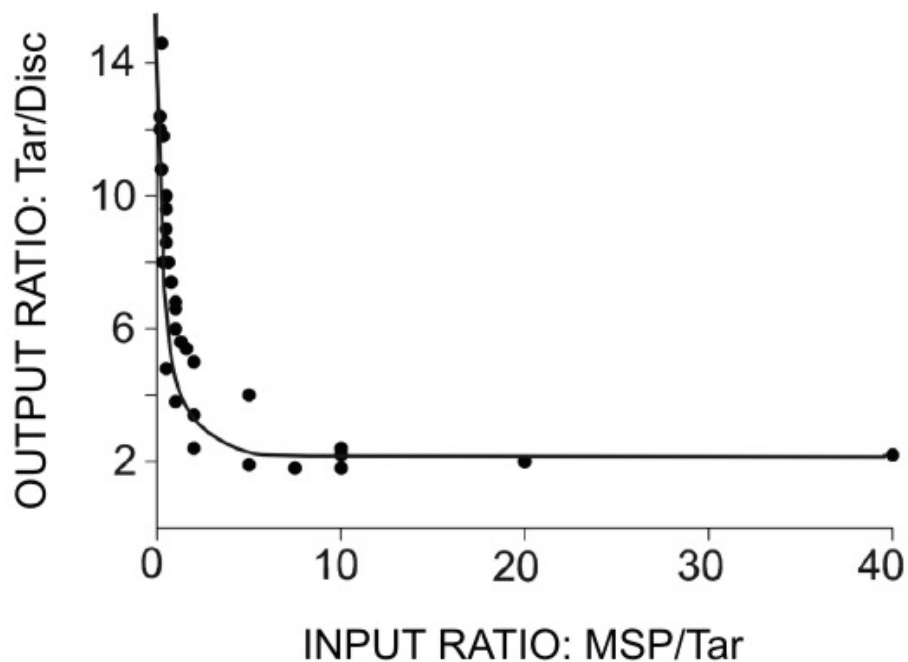


Figure 7. Receptor Molecules per Nanodisc. The input ratio of MSP/Tar in nanodisc assembly mixtures was varied over a wide range (while the ratio MSP/lipid was kept constant). The resulting receptor nanodiscs were analyzed for relative content of MSP and Tar by SDS-PAGE. The plot shows the relationship between input and output ratio. Note: output ratio is expressed in Tar monomers/nanodisc; 2 MSP monomers are necessary to form a nanodisc.

Receptor Modification

Receptor nanodisc preparations were tested for the ability of Tar to be covalently modified. The preparations were incubated in parallel assays with the methyltransferase CheR and deamidase CheB. Conditions were chosen such that maximal modification would occur. Under these conditions the extent of modification provides a measure of receptor cytoplasmic domains which are correctly folded and accessible to the modification enzymes. Tar carries four sites which are subject to modification. In the unmodified state the modification two of these sites are present as glutamates and are available for methylation, and two of these sites are present as glutamines and are available for deamidation. The extent of modification can be quantified by immunoblotting, because methylated receptor migrates with an apparent lower molecular weight and deamidated receptor migrates with an apparent higher molecular weight relative to unmodified receptor. Figure 8 provides an example of this analysis. Shown are samples of Tar in membrane vesicles, purified in detergent and incorporated into nanodiscs with increasing numbers of receptor molecules per nanodisc. For each sample unmodified material was included, to indicate the position of unmodified Tar and to demonstrate that the analysis is not impaired by the presence of any degradation bands. The result is expressed as the percent of receptor in a modified position relative to the total amount of receptor in the respective lane. Tar in membrane vesicles is typically methylated to about 40% and deamidated to 50%, consistent with the notion that about half of the receptor in the vesicles is oriented inside out. The difference in the results for methylation and deamidation is reproducible; the reasons for the difference are unknown. Tar purified in detergent is incapable of modification. In stark contrast Tar in nanodiscs is readily modified. For nanodiscs with a low number of receptor molecules incorporated, methylation is about 60% and deamidation 75%. The modification is increased relative to membrane vesicles consistent with the idea that receptor cytoplasmic domains which were sequestered in the vesicles became accessible. The modification data for all nanodisc preparations are summarized in Figure 9, the upper panel (A) shows deamidation data, the lower panel (B) methylation data. Both types of modification exhibit the very same pattern. The modification is maximal and constant for preparations which carry on average one to three receptor dimers per disc. As the number of receptor molecules per disc increases further, the modification decreases. It appears likely that, as the number of receptor molecules increases, the receptor dimers have to pack more densely which reduces the accessibility of

the modification sites for the modification enzymes. The results support the notion that receptor dimers are the functional units in respect of receptor modification.

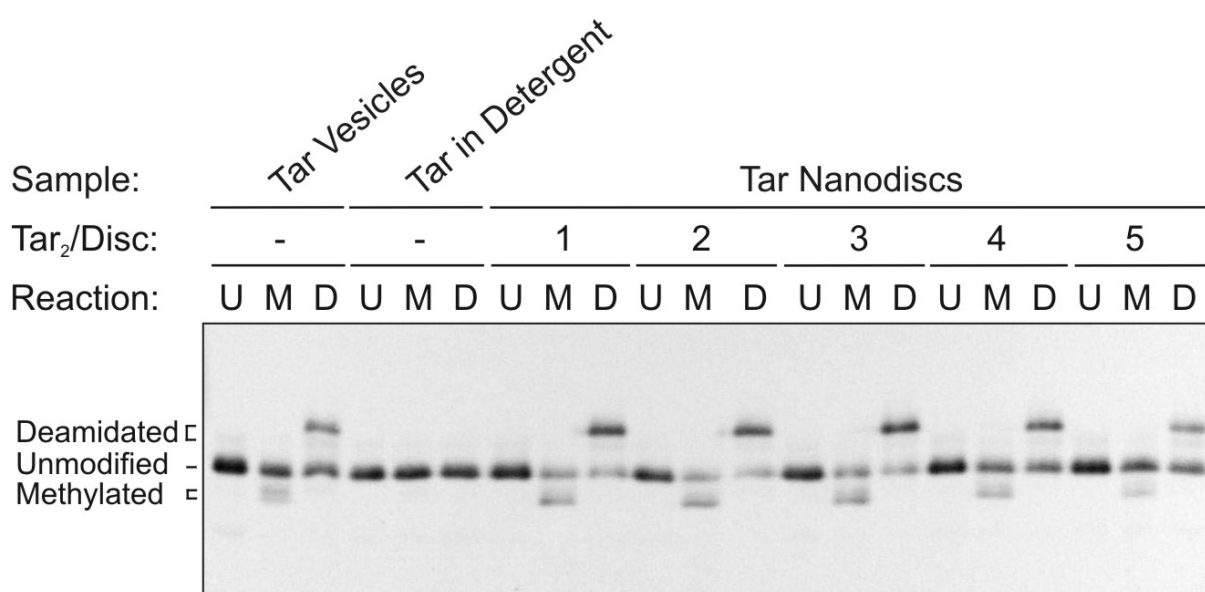


Figure 8. Receptor Modification. Receptor preparations were subjected to enzymatic methylation (M) and demethylation (D) reactions and analyzed by immunoblotting. The figure shows representative examples as indicated. For each preparation an unmodified sample which was not subjected to a reaction (U) was included to test for degradation. Positions of the respective receptor bands are indicated to the right.

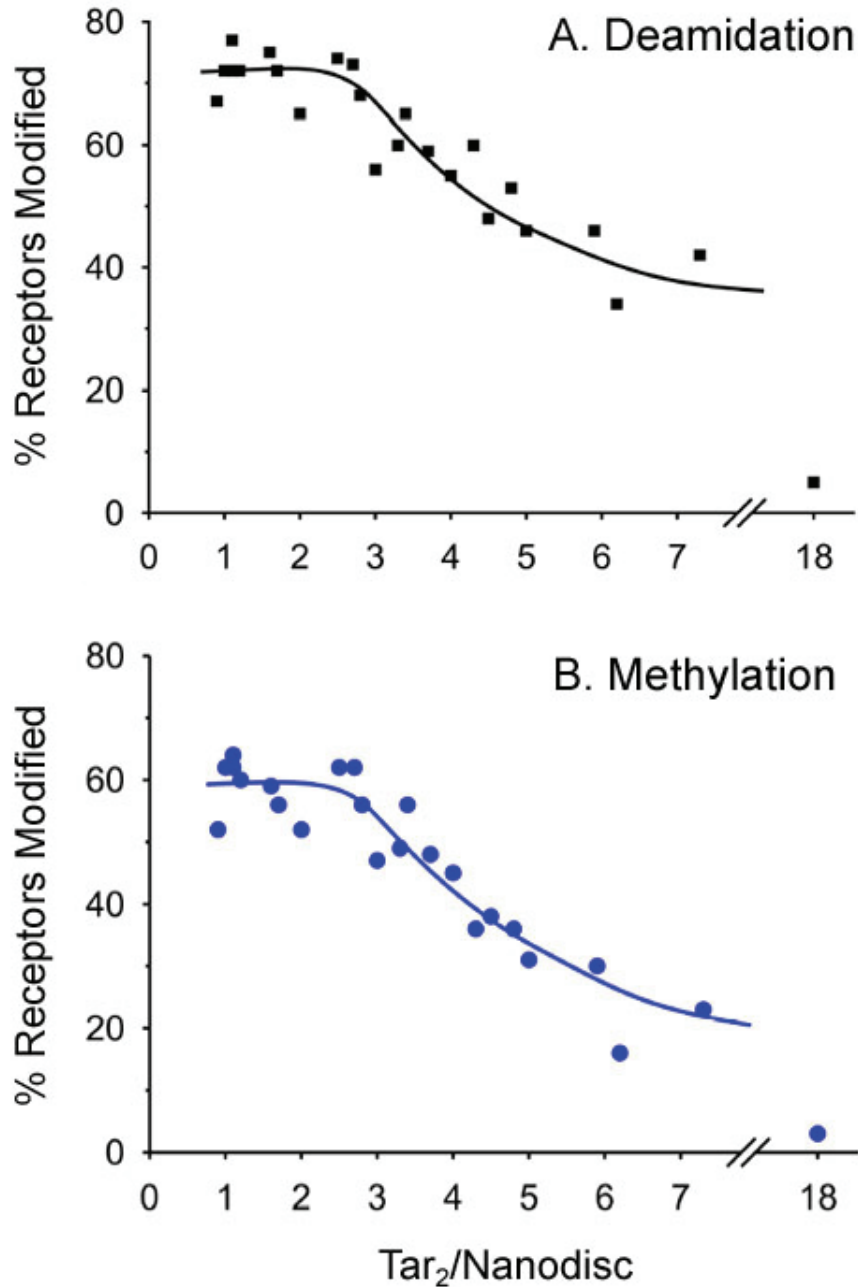


Figure 9. Receptor Modification Results. Immunoblots from modification assays (Fig. 8) were digitized and quantified for the relative amount of receptor modified. The plots summarize the results for deamidation (A) and methylation (B) for all Tar nanodisc preparations.

Kinase activation

Receptor nanodisc preparations were tested for their ability to activate the kinase CheA and to modulate the CheA activity in a ligand dependent fashion. Receptor preparations, CheA, CheW and CheY were preincubated to form signaling complexes, reactions were initiated by addition of radiolabeled ATP. Parallel reactions were performed in absence and presence of aspartate. The formation of phospho-CheY was monitored by SDS-PAGE and phosphorimaging, an example is shown in Figure 10. The upper part displays a Coomassie Blue stained gel, the lower part a phosphorimage of the CheY region of the gel. Tar in vesicles activates the kinase well, and presence of ligand reduces this activity to a level as low as the activity of CheA in the absence of receptor. Activation of kinase does not occur with detergent solubilized receptor. Tar in the nanodiscs preparations is capable of CheA activation as well as CheA inhibition in the presence ligand. The ability to stimulate kinase is dependent on the number of receptor dimers incorporated in the nanodiscs. Bands from the phosphoimage were quantified; results were adjusted for autophosphorylation activity in the absence of receptor and normalized to the activity of Tar in vesicles. Figure 11 summarizes the kinase activation data for all preparations. Kinase activation is very low for nanodiscs which have on average one receptor dimer incorporated; it increases as the number of receptor dimers per nanodisc increases and reaches a maximum for nanodiscs which have on average three receptor dimers incorporated. For nanodiscs with more receptor molecules incorporated the activity drops, presumably because the three receptor dimers cannot assume a conformation which is optimal for kinase activation. These observations provide evidence that trimers of receptor dimers are the functional units for activating kinase. For all receptor nanodiscs preparations inhibition of kinase in the presence of ligand occurred to a level as low for receptor vesicles in presence of ligand. The assay can only demonstrate inhibition of kinase from the activity level present in the absence of ligand. The results suggest that all receptor in a nanodiscs preparation, which is capable of kinase activation is also capable of ligand binding and transmembrane signaling. However, for receptor which does not participate in kinase activation in these assays no judgement about the ability for ligand binding and transmembrane signaling can be made.

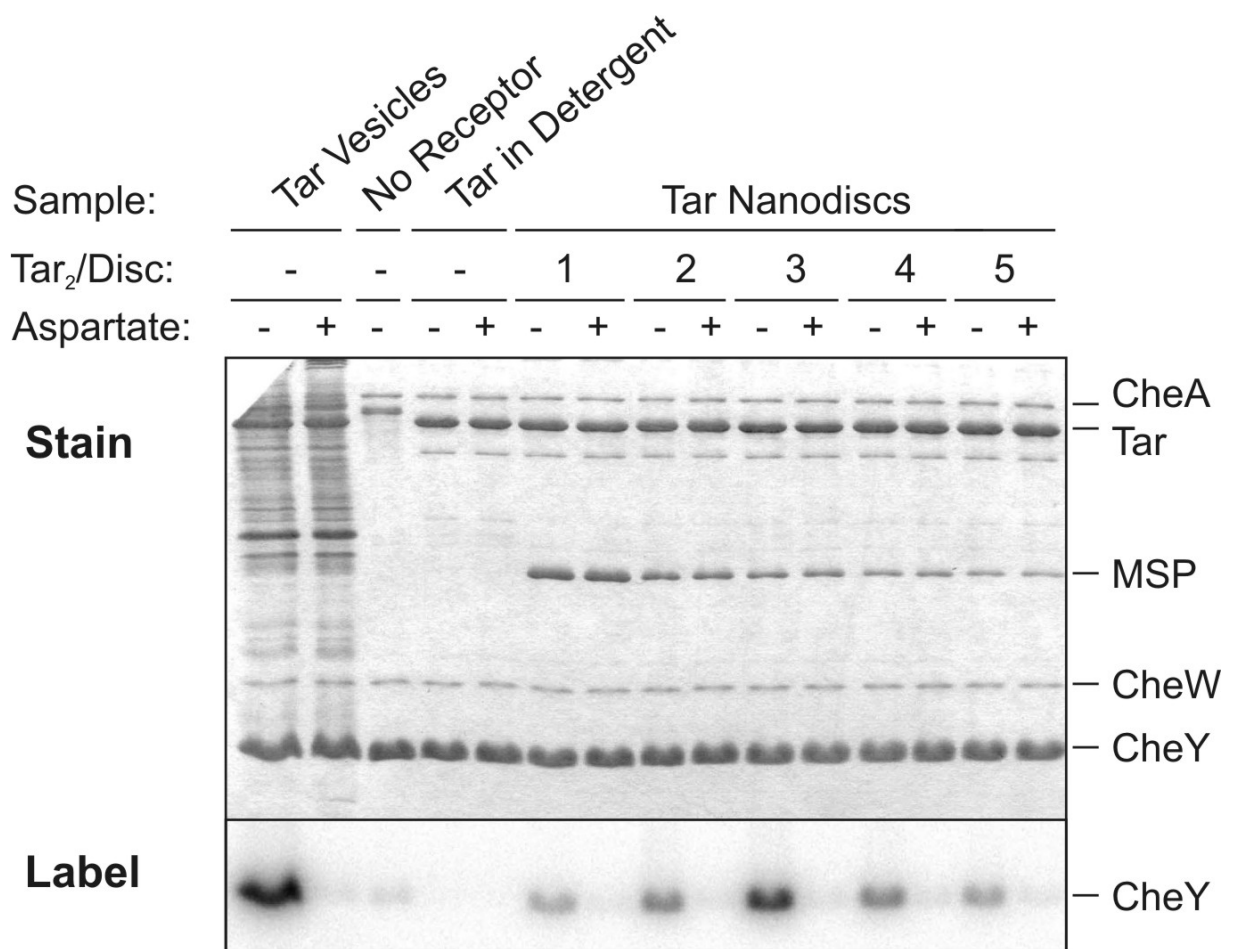


Figure 10. Kinase Activation and Inhibition. Receptor preparations were subjected to coupled kinase assays and analyzed by SDS-PAGE and phosphorimaging. The upper part (Stain) displays a Coomassie Blue stained gel, the lower part (Label) the corresponding phosphorimage. Shown are representative samples as indicated. Positions of proteins are indicated to the right. Parallel assays without and with ligand (aspartate) were performed to test kinase activation and inhibition, a sample without receptor was included to assess autophosphorylation.

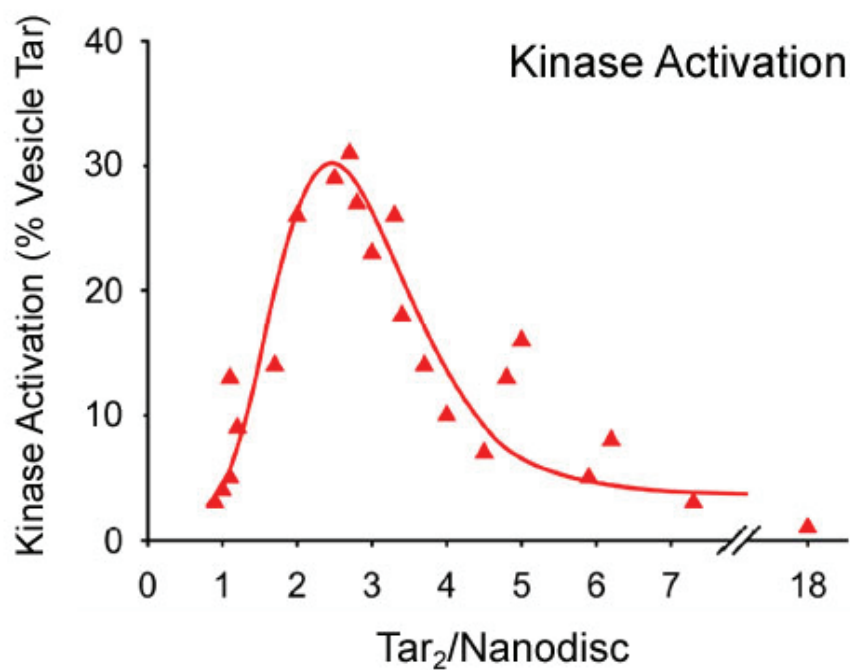


Figure 11. Kinase Activation Results. Phosphoimages from kinase assays (Fig. 10) were quantified; results were adjusted for autophosphorylation and normalized to Tar vesicles. The plot summarizes the results for all Tar nanodisc preparations.

Ligand Binding and Transmembrane Signaling

Chemoreceptor methylation rates are influenced by the presence of ligand (Terwilliger et al. 1986a). We tested the ability of Tar in nanodiscs to bind ligand and carry out transmembrane signaling by measuring initial rates of methylation in presence and absence of aspartate. The experiments described to test for the ability of receptor to be modified were designed to determine maximal modification rather than modification rates. For the measurement of initial methylation rates we employed a lower methyltransferase concentration and used radiolabeled S-adenosyl methionine. At various times samples were taken and the amount of label incorporated into receptor was determined. The measured rates were normalized to the rate of Tar in vesicles in the absence of aspartate. We tested Tar nanodisc preparations with an average of one receptor dimer per disc and preparations with on average three receptor dimers per disc; the results are shown in Figure 12. Tar in vesicles exhibits a two-fold increase in the methylation rate in the presence of aspartate. Both Tar nanodisc preparations show the same two-fold stimulation of methylation in the presence of aspartate, which indicates that receptor incorporated into nanodiscs is fully capable of ligand binding and transmembrane signaling. The ability of ligand binding and signaling is independent of the number of receptor dimers incorporated into a nanodisc.

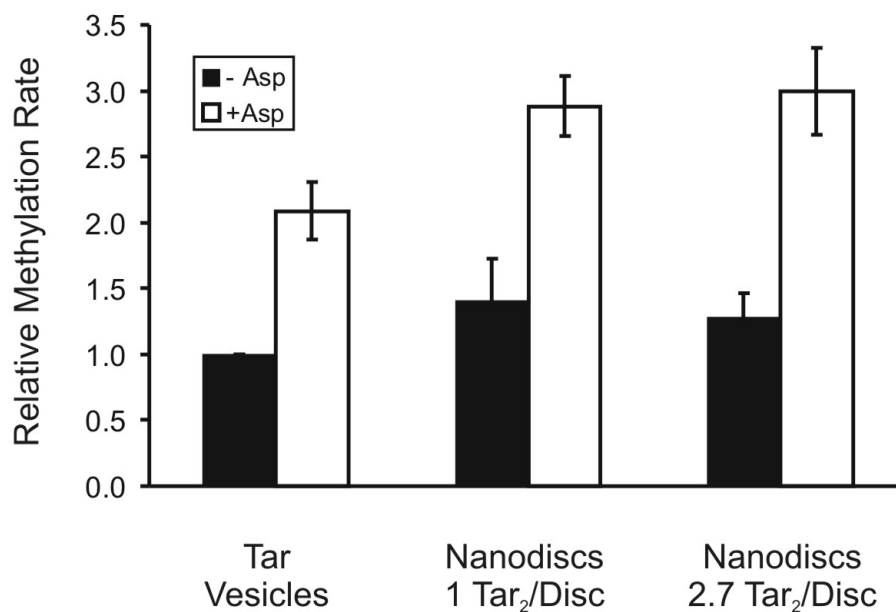


Figure 12. Relative Methylation Rates. Initial rates of methylation in absence and presence of ligand (Asp) were determined for the samples indicated. Results from three independent experiments were averaged and normalized to rate of methylation of Tar vesicles in absence of ligand. Error bars are standard deviations.

Discussion

We investigated the relationship between functional activities of chemoreceptor Tar and its oligomeric state. In a novel approach we solubilized and purified receptor in nanodiscs. The approach allowed us to reconstitute receptor in a native lipid environment while at the same time controlling the oligomeric state of the receptor. We prepared receptor nanodiscs from receptor purified in detergent, detergent-solubilized *E. coli* lipids and MSP. The formation of nanodiscs was initiated by removal of detergent and receptor nanodiscs were purified on a Ni-column utilizing the His-tag on the receptor. Receptor remained in solution after removal of detergent and a fraction of MSP was retained with receptor on the Ni-column, indicating successful formation of receptor nanodiscs. The formation of receptor nanodiscs was confirmed by size exclusion chromatography. A set of receptor nanodiscs with a varying number of receptor dimers incorporated was produced by varying the ratio of receptor and disc components in the assembly mixture. This provided us with a way to control and study the oligomeric state of receptor.

Varying the input ratios of Tar and disc components yielded a set of receptor nanodiscs with a varying output ratio of Tar/disc (Fig. 7). For several preparations a high input ratio of MSP/Tar, i.e. excess of disc components over Tar, was employed. For these preparations the output ratio reached a minimum of 2 Tar/disc. Receptor molecules inserted into discs as dimers and exist in dimeric form in the detergent purified state. Receptor dimers do not associate to a higher oligomeric state in detergent and insert independently into nanodiscs. Intermediate input ratios produced non-integral output ratios. In each preparation a distribution of Tar/disc is produced, as is expected for independent insertion of molecules. Receptor dimers which are confined in a nanodisc can associate into a higher oligomeric state through diffusion as illustrated in Figure 13A. A consequence of independent insertion of receptor dimers is random orientation of the receptor dimers relative to each other. Only a fraction of the preparation will have all receptor dimers inserted parallel and competent to assume the oligomeric state suggested by the output ratio. Each receptor can assume one of two orientations, the possible combinations of three receptor dimers which inserted independently and randomly are illustrated in Figure 13 B. For $n=3$ receptor dimers inserting into one nanodisc $2^n=8$ possible combinations of orientations exist. Only for 2 of these combinations all receptor dimers are oriented parallel and competent for forming a trimer of dimers. Thus, if a

receptor function is dependent on the oligomeric state of the receptor, the corresponding activity must be expected to be lowered accordingly.

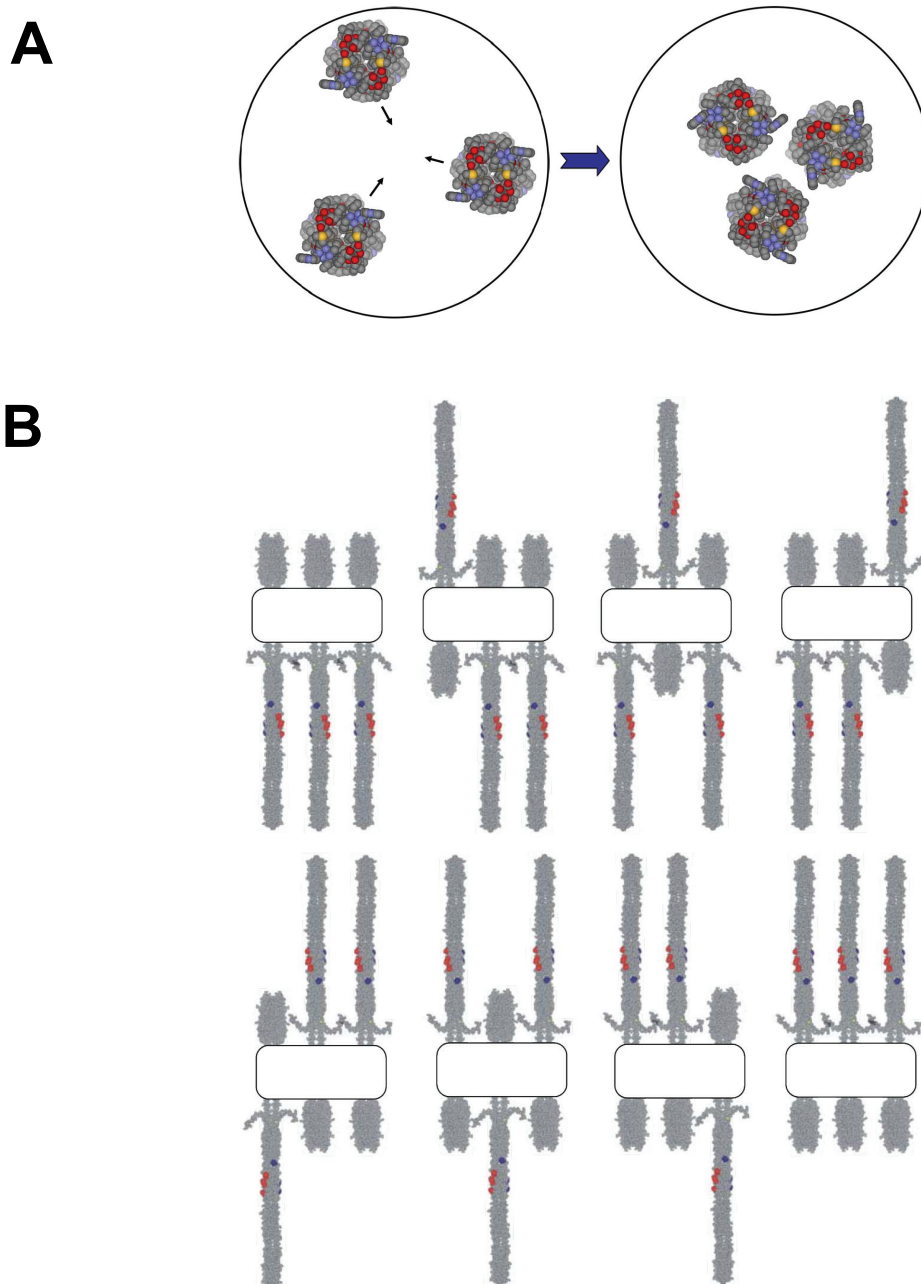


Figure 13. Formation of Receptor Oligomers. Receptor dimers insert independently into nanodiscs as illustrated for 3 receptor dimers. Receptor dimers can freely diffuse in nanodiscs to form an oligomer (A). Required for oligomer formation is that receptors insert into nanodiscs in the same orientation. Receptors insert into nanodiscs with random orientation (B). For three receptor dimers two combinations exist in which the three dimers are inserted parallel and are able to form a trimer.

Nanodisc preparations were subjected to enzymatic assays to access the ability of the receptors to be covalently modified through methylation and deamidation and to activate the kinase. While receptor in the detergent-purified state is inactive in all three of these functions (see Figures 8 and 10), the activity is regained in nanodiscs. For comparison the results of the different assays are summarized in Figure 14. The two modification activities exhibit the very same pattern. Modification is constant and maximal for nanodiscs with 1-3 dimers inserted. Isolated receptor dimers are readily modified and modification does not depend on the oligomeric state. Modification activity decreases as more dimers are inserted. In contrast kinase activation shows a very different pattern. It is maximal for preparations which have on average three dimers inserted into one nanodisc. Three receptor dimers, most likely associated to a trimer of dimers, are required for kinase activation. The existence of trimers of dimers has been suggested by the crystal structure of a receptor cytoplasmic fragment (Kim et al. 1999), from *in vivo* cross-linking experiments (Studdert and Parkinson 2004) and from the cellular stoichiometry of the signaling complex (Li and Hazelbauer 2004). Our results are consistent with the existence of trimers and provide a functional interpretation. At the maximum, kinase activation in nanodiscs does not reach the level of vesicles, which is expected for random insertion of receptor dimers (see above). As the number of dimers incorporated deviates from 3 the kinase activation decreases. Nanodiscs carrying only single receptor dimers are unable to activate kinase. All activities decrease as the number of dimers per disc increases further. Receptors have to pack more densely which prohibits access of the modification enzymes to the sites of modification, and receptors are forced into a conformation which does not allow kinase activation.

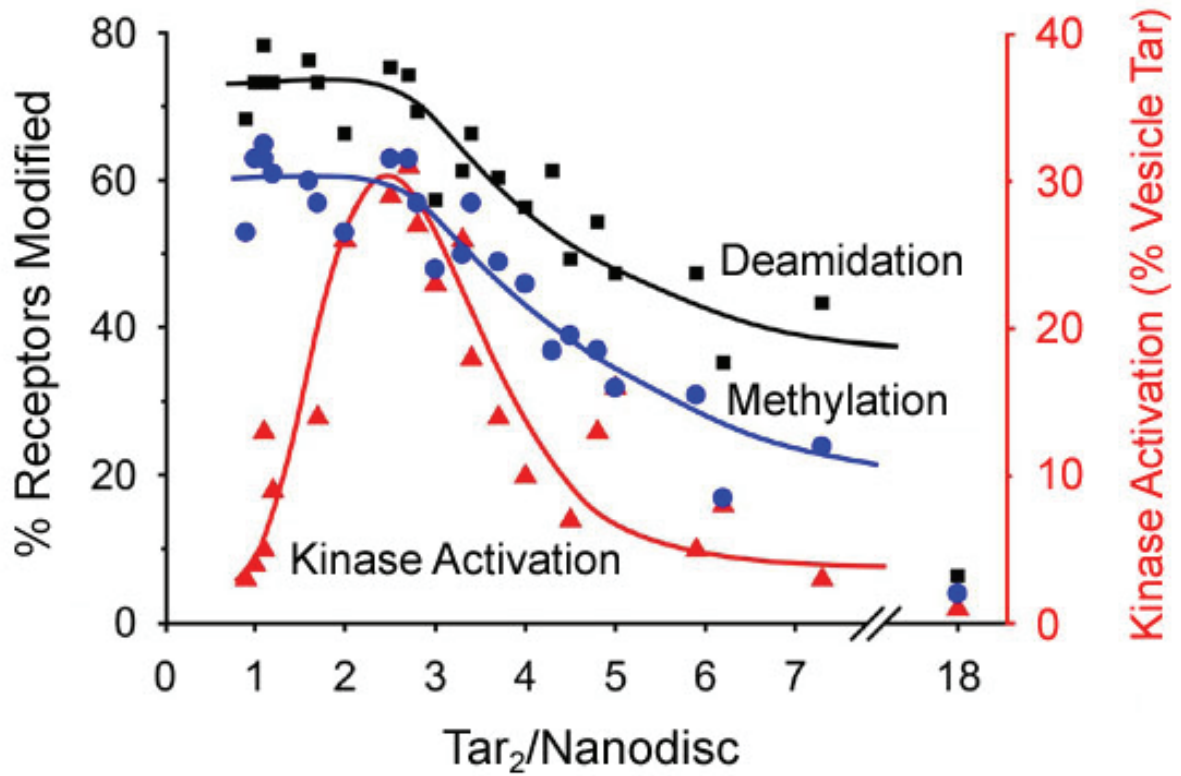


Figure 14. Summary Receptor Activity in Nanodiscs. For comparison data from deamidation (Fig. 9A), methylation (Fig. 9B) and kinase activation (Fig 11) are combined in one plot. The modification activities deamidation and methylation show the very same patterns: maximal modification for nanodiscs with 1-3 dimers inserted. In striking contrast kinase activation is maximal for 3 receptor dimers per nanodisc.

The ability of receptor to bind ligand and perform transmembrane signaling was tested by assessing kinase inhibition caused by the presence of ligand (Fig 10). In these assays kinase inhibition occurred for all receptor nanodisc preparations to a level as low as for receptor vesicles indicating that receptor is competent in these functions. However, the assays can only demonstrate these functions well for preparations which show high kinase activation. For preparations with low initial kinase activation, as is the case for nanodisc preparations with single dimers, no conclusion can be made. Therefore we also assessed the change in methylation rates caused by the presence of ligand for nanodiscs which carry on average one receptor dimer and nanodiscs which carry on average three receptor dimers (Figure 12). Both preparations showed the same two-fold increase in methylation in the presence of ligand as the vesicle control. Thus, ligand binding and transmembrane signaling are functions which are carried by receptor dimers. These functions occur to the same extent in a higher oligomeric state, but they do not depend on a higher oligomeric state.

We suggest the following correlation between chemoreceptor function and oligomeric state as illustrated in Figure 15: the lowest oligomeric state which chemoreceptors assume is the dimeric state. Receptors dimers are competent in the functions ligand binding, transmembrane signaling and adaptational modification. These functions are not impaired as receptors assume a higher oligomeric state. Isolated receptor dimers are not capable of kinase activation. Kinase activation requires a trimer of dimers.

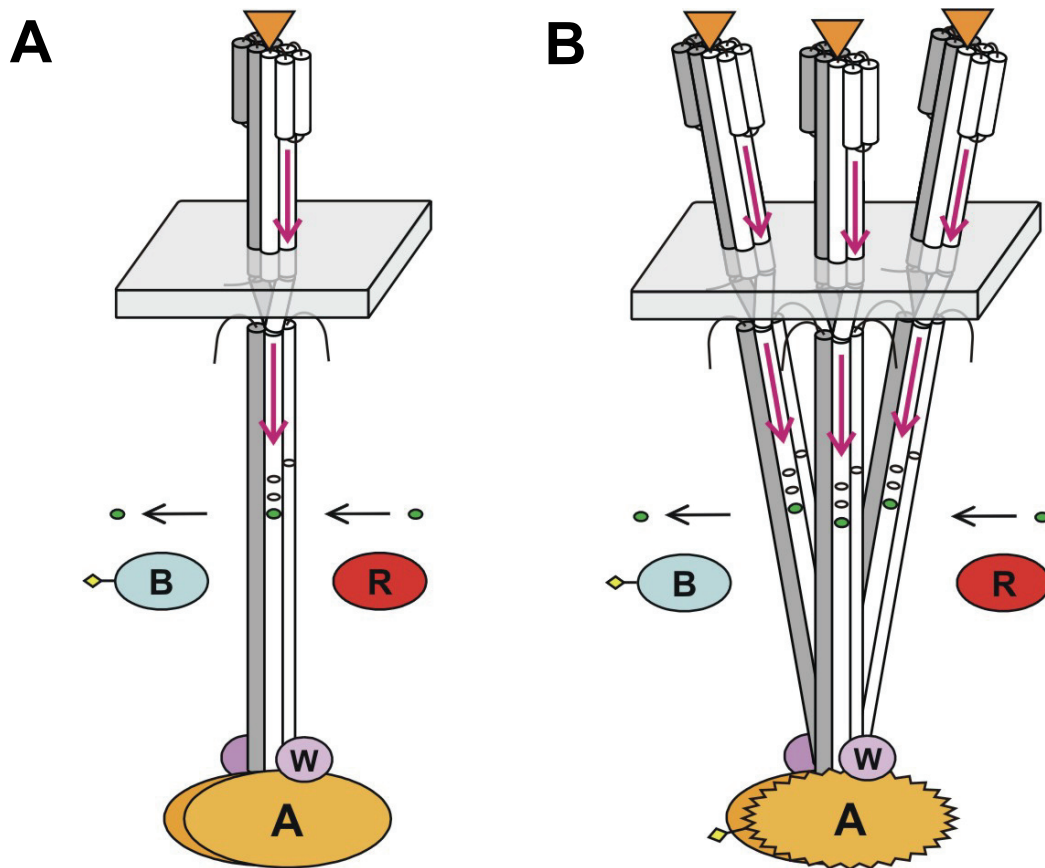


Figure 15. Correlation of Oligomeric State and Function. Isolated receptor dimers (A) are efficient at ligand binding, transmembrane signaling and adaptational modification, but they are inefficient in kinase activation. Trimers of receptor dimers (B) are required for kinase activation. Dimers in a trimer of dimers exhibit all functions of isolated dimers.

Concluding Remarks

This thesis explores specific aspects of chemoreceptor organization and function to increase the understanding of signal transduction in *Escherichia coli*.

Membrane boundaries of chemoreceptors were thus far deduced from sequence. Chapter 1 presents an experimental determination of the hydrophilic/hydrophobic boundaries of a chemoreceptor. To determine the membrane boundaries the accessibility of introduced cysteines to a hydrophilic sulfhydryl reagent was assessed. Membrane boundaries were found to be located interior to the charged residues which bracket the segments of hydrophobic residues. Charged residues are commonly found at one or both ends of putative transmembrane segments and thus the displacement of the boundaries from the charged residues is noteworthy. Determination of the membrane boundaries provided means of aligning the two transmembrane segments and indicated that the receptor is oriented normal to the plane of the membrane.

Chemoreceptors have been described as homodimers which can form trimers and also higher order arrays. While some receptor functions are attributed to a particular oligomeric state of the receptor, a rigorous direct correlation between oligomeric states and functions has not been defined as it requires isolation of receptor in defined oligomeric states. The study presented in chapter 2 provides a correlation of oligomeric state and function. Chemoreceptors were solubilized and isolated in nanodiscs, nanoscale discs of lipid bilayer, at a controlled number of receptor molecules per disc. The receptor nanodisc preparations were subjected to enzymatic assays which showed that isolated receptor dimers bind ligand, perform transmembrane signaling and are readily modified, but are not able to activate kinase. Activation of kinase and control of kinase activity requires a trimer of receptor dimers. The study demonstrated that functional activities of chemoreceptors are dependent on the oligomeric state.

The studies in this thesis not only provide valuable information for understanding chemotactic signaling in *E. coli*, they also describe new techniques which are of wide interest for studying membrane proteins. The accessibility approach used for determination of membrane boundaries in chapter 1 is minimally perturbing and does not require specialized equipment. Membrane boundaries are defined only for relatively few proteins, the presented technique provides a convenient method applicable to other

membrane proteins. The solubilization of proteins in nanodiscs is a novel technology to isolate membrane proteins in a native bilayer environment and study them as individual entities. In chapter 2 this technology was adapted to study the oligomeric state of chemoreceptors, a new approach which is generally applicable to study the oligomeric state of membrane proteins. The successful use of these techniques in the presented thesis should provide a strong motivation for applying them to other membrane proteins.

References

- Abramson, J., Smirnova, I., Kasho, V., Verner, G., Kaback, H.R., and Iwata, S. 2003. Structure and mechanism of the lactose permease of *Escherichia coli*. *Science* **301**: 610-615.
- Adler, J. 1969. Chemoreceptors in bacteria. *Science* **166**: 1588-1597.
- Altenbach, C., Greenhalgh, D.A., Khorana, H.G., and Hubbell, W.L. 1994. A collision gradient method to determine the immersion depth of nitroxides in lipid bilayers: application to spin-labeled mutants of bacteriorhodopsin. *Proc. Natl. Acad. Sci. USA* **91**: 1667-1671.
- Barnakov, A., Altenbach, C., Barnakova, L., Hubbell, W.L., and Hazelbauer, G.L. 2002. Site-directed spin labeling of a bacterial chemoreceptor reveals a dynamic, loosely packed transmembrane domain. *Protein Sci.* **11**: 1472-1481.
- Barnakov, A.N., Barnakova, L.A., and Hazelbauer, G.L. 1998. Comparison *in vitro* of a high- and a low-abundance chemoreceptor of *Escherichia coli*: similar kinase activation but different methyl-accepting activities. *J. Bacteriol.* **180**: 6713-6718.
- Barnakov, A.N., Barnakova, L.A., and Hazelbauer, G.L. 1999. Efficient adaptational demethylation of chemoreceptors requires the same enzyme-docking site as efficient methylation. *Proc. Natl. Acad. Sci. USA* **96**: 10667-10672.
- Bass, R.B., Coleman, M.D., and Falke, J.J. 1999. Signaling domain of the aspartate receptor is a helical hairpin with a localized kinase docking surface: cysteine and disulfide scanning studies. *Biochemistry* **38**: 9317-9327.
- Bass, R.B., and Falke, J.J. 1998. Detection of a conserved alpha-helix in the kinase-docking region of the aspartate receptor by cysteine and disulfide scanning. *J. Biol. Chem.* **273**: 25006-25014.
- Bayburt, T., Grinkova, Y., and Sligar, S. 2002. Self-Assembly of Discoidal Phospholipid Bilayer Nanoparticles with Membrane Scaffold Proteins. *Nano. Lett.* **2**: 853-856.
- Bayburt, T.H., and Sligar, S.G. 2003. Self-assembly of single integral membrane proteins into soluble nanoscale phospholipid bilayers. *Protein Sci.* **12**: 2476-2481.
- Berg, H.C. 2003. The rotary motor of bacterial flagella. *Annu. Rev. Biochem.* **72**.
- Bibikov, S.I., Biran, R., Rudd, K.E., and Parkinson, J.S. 1997. A signal transducer for aerotaxis in *Escherichia coli*. *J. Bacteriol.* **179**: 4075-4079.
- Blair, D.F. 1995. How bacteria sense and swim. *Annu. Rev. Microbiol.* **49**: 489-522.

- Bollinger, J., Park, C., Harayama, S., and Hazelbauer, G.L. 1984. Structure of the Trg protein: Homologies with and differences from other sensory transducers of *Escherichia coli*. *Proc. Natl. Acad. Sci. USA* **81**: 3287-3291.
- Borkovich, K.A., Kaplan, N., Hess, J.F., and Simon, M.I. 1989. Transmembrane signal transduction in bacterial chemotaxis involves ligand-dependent activation of phosphate group transfer. *Proc. Natl. Acad. Sci. USA* **86**: 1208-1212.
- Bren, A., and Eisenbach, M. 2000. How signals are heard during bacterial chemotaxis: protein-protein interactions in sensory signal propagation. *J. Bacteriol.* **182**: 6865-6873.
- Burrows, G.G., Newcomer, M.E., and Hazelbauer, G.L. 1989. Purification of receptor protein Trg by exploiting a property common to chemotactic transducers of *Escherichia coli*. *J. Biol. Chem.* **264**: 17309-17315.
- Butler, S.L., and Falke, J.J. 1998. Cysteine and disulfide scanning reveals two amphiphilic helices in the linker region of the aspartate chemoreceptor. *Biochemistry* **37**: 10746-10756.
- Chelsky, D., Gutterson, N.I., and Koshland, D.E., Jr. 1984. A diffusion assay for detection and quantitation of methyl-esterified proteins on polyacrylamide gels. *Anal. Biochem.* **141**: 143-148.
- Chen, X., and Koshland, D.E., Jr. 1995. The N-terminal cytoplasmic tail of the aspartate receptor is not essential in signal transduction of bacterial chemotaxis. *J. Biol. Chem.* **270**: 24038-24042.
- Chervitz, S.A., Lin, C.M., and Falke, J.J. 1995. Transmembrane signaling by the aspartate receptor: engineered disulfides reveal static regions of the subunit interface. *Biochemistry* **34**: 9722-9733.
- Danielson, M.A., Bass, R.B., and Falke, J.J. 1997. Cysteine and disulfide scanning reveals a regulatory alpha-helix in the cytoplasmic domain of the aspartate receptor. *J. Biol. Chem.* **272**: 32878-32888.
- Denisov, I., Grinkova, Y., Lazarides, A., and Sligar, S. 2004. Directed self-assembly of monodisperse phospholipid bilayer Nanodiscs with controlled size. *J. Am. Chem. Soc.* **126**: 3477-3487.
- Duan, H., Civjan, N., Sligar, S., and Schuler, M. 2004. Co-incorporation of heterologously expressed Arabidopsis cytochrome P450 and P450 reductase into soluble nanoscale lipid bilayers. *Arch. Biochem. Biophys.* **424**: 141-153.

- Engelman, D.M., Steitz, T.A., and Goldman, A. 1986. Identifying nonpolar transbilayer helices in amino acid sequences of membrane proteins. *Ann. Rev. Biophys. Biophys. Chem.* **15**: 321-353.
- Falke, J.J., Bass, R.B., Butler, S.L., Chervitz, S.A., and Danielson, M.A. 1997. The two-component signaling pathway of bacterial chemotaxis: a molecular view of signal transduction by receptors, kinases, and adaptation enzymes. *Annu. Rev. Cell Dev. Biol.* **13**: 457-512.
- Falke, J.J., and Hazelbauer, G.L. 2001. Transmembrane signaling in bacterial chemoreceptors. *Trends Biochem. Sci.* **26**: 257-265.
- Falke, J.J., and Kim, S.H. 2000. Structure of a conserved receptor domain that regulates kinase activity: the cytoplasmic domain of bacterial taxis receptors. *Curr. Opin. Struct. Biol.* **10**: 462-469.
- Feng, X., Baumgartner, J.W., and Hazelbauer, G.L. 1997. High- and low-abundance chemoreceptors in *Escherichia coli*: differential activities associated with closely related cytoplasmic domains. *J. Bacteriol.* **179**: 6714-6720.
- Feng, X., Lilly, A.A., and Hazelbauer, G.L. 1999. Enhanced function conferred on low-abundance chemoreceptor Trg by a methyltransferase-docking site. *J. Bacteriol.* **181**: 3164-3171.
- Gegner, J.A., Graham, D.R., Roth, A.F., and Dahlquist, F.W. 1992. Assembly of an MCP receptor, CheW, and kinase CheA complex in the bacterial chemotaxis signal transduction pathway. *Cell* **70**: 975-982.
- Hazelbauer, G.L. 2004. Bacterial chemotaxis: A model for sensory receptor systems. In *Encyclopedia of Neuroscience*, 3rd ed. (eds. G. Adelman, and B.H. Smith). Elsevier., Amsterdam, The Netherlands. CD-ROM.
- Hess, J.F., Oosawa, K., Kaplan, N., and Simon, M.I. 1988. Phosphorylation of three proteins in the signaling pathway of bacterial chemotaxis. *Cell* **53**: 79-87.
- Hughson, A.G., Lee, G.F., and Hazelbauer, G.L. 1997. Analysis of protein structure in intact cells: crosslinking *in vivo* between introduced cysteines in the transmembrane domain of a bacterial chemoreceptor. *Protein Sci.* **6**: 315-322.
- Jones, D.T., Taylor, W.R., and Thornton, J.M. 1994. A model recognition approach to the prediction of all-helical membrane protein structure and topology. *Biochemistry* **33**: 3038-3049.

- Kehry, M.R., Bond, M.W., Hunkapiller, M.W., and Dahlquist, F.W. 1983a. Enzymatic deamidation of methyl-accepting chemotaxis proteins in *Escherichia coli* catalyzed by the *cheB* gene product. *Proc. Natl. Acad. Sci. USA* **80**: 3599-3603.
- Kehry, M.R., Engström, P., Dahlquist, F.W., and Hazelbauer, G.L. 1983b. Multiple covalent modifications of Trg, a sensory transducer of *Escherichia coli*. *J. Biol. Chem.* **258**: 5050-5055.
- Kim, K.K., Yokota, H., and Kim, S.-H. 1999. Four-helical-bundle structure of the cytoplasmic domain of a serine chemotaxis receptor. *Nature* **400**: 787-792.
- Kim, S.-H., Wang, W., and Kim, K.K. 2002. Dynamic and clustering model of bacterial chemotaxis receptors: Structural basis for signaling and high sensitivity. *Proc. Natl. Acad. Sci. USA* **99**: 11611–11615.
- Lai, W.-C., and Hazelbauer, G.L. 2005. Carboxyl-terminal extensions beyond the conserved pentapeptide reduce rates of chemoreceptor adaptational modification. *J. Bacteriol.* **187**: 5115-5121.
- Lai, W.-C., Peach, M.L., Lybrand, T.P., and Hazelbauer, G.L. 2006. Diagnostic cross-linking of paired cysteine pairs demonstrates homologous structures for two chemoreceptor domains with low sequence identity. *Protein Sci.* **15**: 94-101.
- Le Moual, H., and Koshland, D.E., Jr. 1996. Molecular evolution of the C-terminal cytoplasmic domain of a superfamily of bacterial receptors involved in taxis. *J. Mol. Biol.* **261**: 568-585.
- Lee, G.F., Burrows, G.G., Lebert, M.R., Dutton, D.P., and Hazelbauer, G.L. 1994. Deducing the organization of a transmembrane domain by disulfide cross-linking. The bacterial chemoreceptor Trg. *J. Biol. Chem.* **269**: 29920-29927.
- Lee, G.F., Dutton, D.P., and Hazelbauer, G.L. 1995. Identification of functionally important helical faces in transmembrane segments by scanning mutagenesis. *Proc. Natl. Acad. Sci. USA* **92**: 5416-5420.
- Lee, G.F., and Hazelbauer, G.L. 1995. Quantitative approaches to utilizing mutational analysis and disulfide crosslinking for modeling a transmembrane domain. *Protein Sci.* **4**: 1100-1107.
- Li, J., Swanson, R.V., Simon, M.I., and Weis, R.M. 1995. The response regulators CheB and CheY exhibit competitive binding to the kinase CheA. *Biochemistry* **34**: 14626-14636.
- Li, M., and Hazelbauer, G.L. 2004. Cellular stoichiometry of the components of the chemotaxis signaling complex. *J. Bacteriol.* **186**: 3687-3694.

- Lin, L.N., Li, J., Brandts, J.F., and Weis, R.M. 1994. The serine receptor of bacterial chemotaxis exhibits half-site saturation for serine binding. *Biochemistry* **33**: 6564-6570.
- Linden, C.D., Blasie, J.K., and Fox, C.F. 1977. A confirmation of the phase behavior of *Escherichia coli* cytoplasmic membrane lipids by X-ray diffraction. *Biochemistry* **16**: 1621-1625.
- Maddock, J.R., and Shapiro, L. 1993. Polar location of the chemoreceptor complex in the *Escherichia coli* cell. *Science* **259**: 1717-1723.
- Milburn, M.V., Prive, G.G., Milligan, D.L., Scott, W.G., Yeh, J., Jancarik, J., Koshland, D.E., Jr., and Kim, S.H. 1991. Three-dimensional structures of the ligand-binding domain of the bacterial aspartate receptor with and without a ligand. *Science* **254**: 1342-1347.
- Milligan, D.L., and Koshland, D.E., Jr. 1988. Site-directed cross-linking. Establishing the dimeric structure of the aspartate receptor of bacterial chemotaxis. *J. Biol. Chem.* **263**: 6268-6275.
- Osborn, M.J., and Munson, R. 1974. Separation of the inner (cytoplasmic) and outer membranes of Gram-negative bacteria. *Methods Enzymol.* **31**: 642-653.
- Pakula, A.A., and Simon, M.I. 1992. Determination of transmembrane protein structure by disulfide cross-linking: the *Escherichia coli* Tar receptor. *Proc. Natl. Acad. Sci. USA* **89**: 4144-4148.
- Parkinson, J.S., and Houts, S.E. 1982. Isolation and behavior of *Escherichia coli* deletion mutants lacking chemotaxis functions. *J. Bacteriol.* **151**: 106-113.
- Peach, M.L., Hazelbauer, G.L., and Lybrand, T.P. 2002. Modeling the transmembrane domain of bacterial chemoreceptors. *Protein Sci.* **11**: 912-923.
- Pfeffer W.F.. 1904. Chemotaxis and Osmotaxis. In *Pflanzenphysiologie. Ein Handbuch der Lehre von Stoffwechsel und Kraftstoffwechsel in der Pflanze*. 2. Aufl., Bd. 2, S. 798-805. Wilhelm Engelmann, Leipzig.
- Rost, B., Casadio, R., Fariselli, P., and Sander, C. 1995. Transmembrane helices predicted at 95% accuracy. *Protein Sci.* **4**: 521-533.
- Schuster, S.C., Swanson, R.V., Alex, L.A., Bourret, R.B., and Simon, M.I. 1993. Assembly and function of a quaternary signal transduction complex monitored by surface plasmon resonance. *Nature* **365**: 343-347.
- Seelig, J., and Seelig, A. 1980. Lipid conformation in model membranes and biological membranes. *Q. Rev. Biophys.* **13**: 19-61.

- Sheridan, R., McCullough, J., and Wakefield, Z. 1971. Phosphoramidic acid and its salts. *Inorganic Syntheses* **13**: 23-26.
- Snyder, M.A., Stock, J.B., and Koshland, D.E., Jr. 1984. Carboxymethyl esterase of bacterial chemotaxis. *Methods Enzymol.* **106**: 321-330.
- Springer, M.S., Goy, M.F., and Adler, J. 1979. Protein methylation in behavioural control mechanisms and in signal transduction. *Nature* **280**: 279-284.
- Stewart, J.B., and Hermodson, M.A. 2003. Topology of RbsC, the membrane component of the *Escherichia coli* ribose transporter. *J. Bacteriol.* **185**: 5234-5239.
- Stock, A.M., Robinson, V.L., and Goudreau, P.N. 2000. Two-component signal transduction. *Annu. Rev. Biochem.* **69**: 183-215.
- Stock, J.B., Clarke, S., and Koshland, D.E., Jr. 1984. The protein carboxymethyltransferase involved in *Escherichia coli* and *Salmonella typhimurium* chemotaxis. *Methods Enzymol.* **106**: 310-321.
- Studdert, G.A., and Parkinson, J.S. 2004. Crosslinking snapshots of bacterial chemoreceptor squads. *Proc. Natl. Acad. Sci. USA* **101**: 2117-2122.
- Terwilliger, T.C., Bollag, G.E., Sternberg, D.W., Jr., and Koshland, D.E., Jr. 1986a. S-methyl glutathione synthesis is catalyzed by the cheR methyltransferase in *Escherichia coli*. *J. Bacteriol.* **165**: 958-963.
- Terwilliger, T.C., Wang, J.Y., and Koshland, D.E., Jr. 1986b. Kinetics of receptor modification. The multiply methylated aspartate receptors involved in bacterial chemotaxis. *J. Biol. Chem.* **261**: 10814-10820.
- Ulmschneider, M.B., and Sansom, M.S. 2001. Amino acid distributions in integral membrane protein structures. *Biochim. Biophys. Acta* **1512**: 1-14.
- von Heijne, G. 1986. The distribution of positively charged residues in bacterial inner membrane proteins correlates with the trans-membrane topology. *EMBO J.* **5**: 3021-3027.
- von Heijne, G. 1992. Membrane protein structure prediction. Hydrophobicity analysis and the positive-inside rule. *J. Mol. Biol.* **225**: 487-494.
- Wadhams, G.H., and Armitage, J.P. 2004. Making sense of it all: Bacterial Chemotaxis. *Nat. Rev. Mol. Cell Biol.* **5**: 1024-1037.
- Weis, R.M., Hirai, T., Chalah, A., Kessel, M., Peters, P.J., and Subramaniam, S. 2003. Electron microscopic analysis of membrane assemblies formed by the bacterial chemotaxis receptor Tsr. *J. Bacteriol.* **185**: 3636-3643.

- Welch, M., Oosawa, K., Aizawa, S., and Eisenbach, M. 1993. Phosphorylation-dependent binding of a signal molecule to the flagellar switch of bacteria. *Proc. Natl. Acad. Sci. USA* **90**: 8787-8791.
- White, S.H., and Wiener, M.C. 1996. The liquid-crystallographic structure of fluid lipid bilayer membranes. In *Biological Membranes: A Molecular Perspective from Computation and Experiment*. (eds. K.M. Merz, Jr., and B. Roux), pp. 127-144. Birkhäuser, Boston.
- Wiener, M.C., and White, S.H. 1992. Structure of a fluid dioleoylphosphatidylcholine bilayer determined by joint refinement of X-ray and neutron diffraction data. III. Complete structure. *Biophys. J.* **61**: 437-447.
- Wu, J., Li, J., Li, G., Long, D.G., and Weis, R.M. 1996. The receptor binding site for the methyltransferase of bacterial chemotaxis is distinct from the sites of methylation. *Biochemistry* **35**: 4984-4993.
- Zhang, P., Bos, E., Heymann, J., Gnaegi, H., Kessel, M., Peters, P.J., and Subramaniam, S. 2004. Direct visualization of receptor arrays in frozen-hydrated sections and plunge-frozen specimens of *E. coli* engineered to overproduce the chemotaxis receptor Tsr. *J. Microsc.* **216**: 76-83.
- Zhulin, I.B. 2001. The superfamily of chemotaxis transducers: from physiology to genomics and back. *Adv. Microb. Physiol.* **45**: 157-198.

Curriculum Vitae

THOMAS BOLDOG

PERSONAL DATA

Date of birth: Feb. 12th, 1973

Place of birth: St. Pölten

Citizenship: Austria

TRAINING

- Sep. 1993 – May 1991 Realistisches Gymnasium Krems Piaristengasse
- Oct. 1991 – May 2001 Masters student in Technical Chemistry at Vienna University of Technology
Subject: Biotechnology, Biochemistry and Food Chemistry
Masters thesis: Analysis of the transmembrane domain of Trg by reactivity of introduced cysteines
Advisors: Dr. C.P. Kubicek, Dr. G.L. Hazelbauer
- Nov. 1997 – Dec. 1998 Washington State University
Research Associate with Dr. G.L. Hazelbauer
- Oct. 1999 – Sep. 2000 Civil Service at Kaiser Franz Joseph Spital, Vienna
Dept. of Clin. Chemistry, Dr. M.M. Müller
- May 2001 – current Doctoral student at Vienna University of Technology
Doctoral thesis: Bacterial chemoreceptors: membrane boundaries and functional correlates of oligomeric state
Advisors: Dr. C.P. Kubicek, Dr. G.L. Hazelbauer
- May 2001 – Dec. 2005 University of Missouri – Columbia
Research Specialist with Dr. G.L. Hazelbauer
- Apr. 2006 – current Boehringer Ingelheim Austria GmbH
Downstream Implementation

INTERNSHIPS

Krems Chemie AG, Aug. 1994
Quality control, Dr. Wertgarner

AWARDS

Stipendium für kurzfristige Aufenthalte im Ausland
Bundesministerium für Bildung, Wissenschaft und Kunst, 1997

PUBLICATIONS

Boldog T., and Hazelbauer G.L. 2004. Accessibility of introduced cysteines in chemoreceptor transmembrane helices reveals boundaries interior to bracketing charged residues. *Protein Sci.*,13:1466-75.

Boldog T., Grimme S., Li, M., Sligar S.G., and Hazelbauer, G.L. 2006. Nanodiscs separate chemoreceptor oligomeric states and reveal their signaling properties. Submitted.

PROFESSIONAL ACTIVITIES

Bacterial Locomotion and Signal Transduction, Research Conference, Cuernavaca, Mexico, Jan. 1999
Poster: Analysis of the transmembrane domain of Trg by reactivity of introduced cysteines to sulfhydryl reagents

Sensory Transduction in Microorganisms, Gordon Research Conference, Ventura, California, Jan. 2002
Poster: Analysis of the transmembrane domain of Trg by reactivity of introduced cysteines to sulfhydryl reagents

Molecular Biology Week, University of Missouri-Columbia, Apr. 2002
Poster: Analysis of the transmembrane domain of Trg by reactivity of introduced cysteines to sulfhydryl reagents

Genetics Area Program, Annual Retreat, University of Missouri-Columbia, Sep. 2002
Poster: Analysis of the transmembrane domain of Trg by reactivity of introduced cysteines to sulfhydryl reagents

Bacterial Locomotion and Signal Transduction, Research Conference, Cuernavaca, Mexico, Jan. 2003
Poster: Determining the boundaries of the transmembrane domain of a chemoreceptor

Missouri Life Sciences Week, University of Missouri-Columbia, Apr. 2003
Poster: Determining the boundaries of the transmembrane domain of a chemoreceptor

Genetics Area Program, Annual Retreat, University of Missouri-Columbia, Sep. 2003
Poster: Analysis of the transmembrane domain of Trg by reactivity of introduced cysteines to sulfhydryl reagents

Sensory Transduction in Microorganisms, Gordon Research Conference, Ventura, California, Jan. 2004
Poster: Accessibility of introduced cysteines in chemoreceptor transmembrane helices reveals boundaries interior to bracketing charged residues

Missouri Life Sciences Week, University of Missouri-Columbia, Apr. 2004
Poster: Accessibility of introduced cysteines in chemoreceptor transmembrane helices reveals boundaries interior to bracketing charged residues

Acknowledgements

My thank goes to Dr. Kubicek for his encouragement to pursue my studies externally and for his support from my alma mater.

I thank Dr. Hazelbauer for inviting me to his laboratory, for introducing me to an exiting field of research and for giving me the opportunity to develop as a scientist.

I thank Dr. Randall for her invaluable advice and for stimulating discussions.

I thank Dr. Li for performing kinetic methylation experiments.

I thank Angela Lilly for site specific mutagenesis of *trg*.